



Radial Velocities of Stars in Globular Clusters: a Look into ω Cen and 47 Tuc

M. Mayor and G. Meylan, Geneva Observatory, Switzerland

Subjected to dynamical investigations since the beginning of the century, globular clusters still provide astrophysicists with theoretical and observational problems, which so far have only been partly solved.

If for a long time the star density projected on the sky was fairly well represented by simple dynamical models, recent

photometry of several clusters reveals a cusp in the luminosity function of the central region, which could be the first evidence for collapsed cores.

The development of photoelectric cross-correlation techniques for the determination of stellar radial velocities opened the door to kinematical investigations (Gunn and Griffin, 1979,

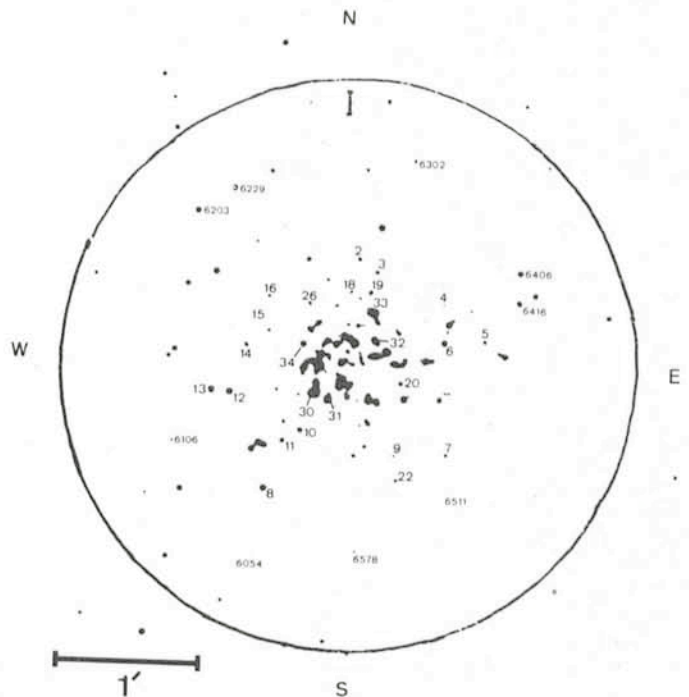
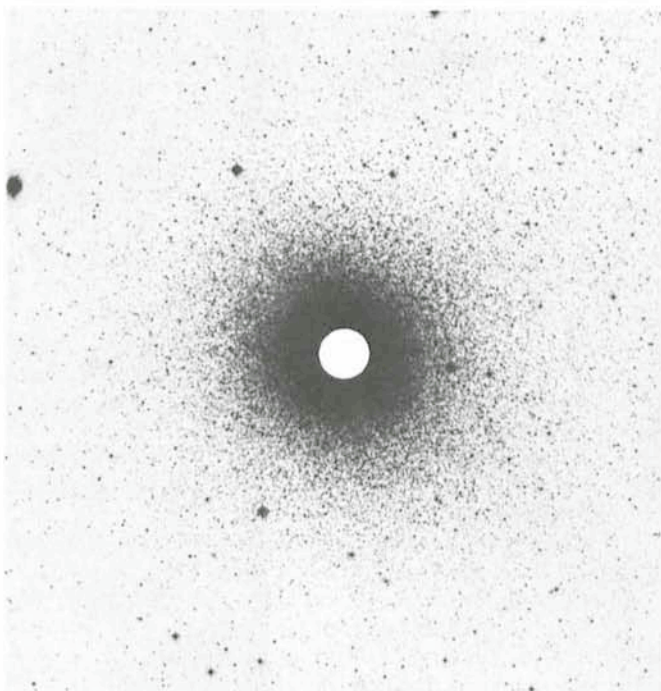


Fig. 1: Left: 47 Tuc (NGC 104) from the Deep Blue Survey – SRC-(J). Right: Centre of 47 Tuc from a near-infrared photometric study of Lloyd Evans. The diameter of the large circle corresponds to the disk of the left photograph. The maximum of the rotation appears inside the circle; the linear part of the rotation curve (solid-body rotation) affects only stars inside one arcminute of the centre.

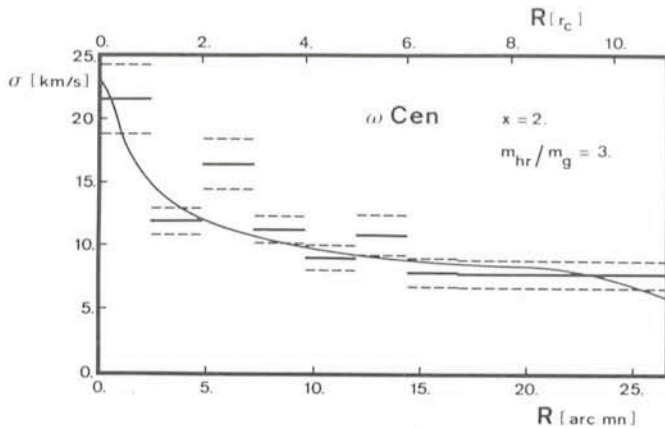


Fig. 4: ω Cen: observed velocity dispersion and model velocity dispersion (continuous line) computed with IMF exponent $x = 2$ and with $m_{hr}/m_g = 3$, where m_{hr} is the mean individual mass of heavy remnants and m_g the individual mass of a giant star.

- (iv) the differential rotation in the outer parts
- (v) the decrease of rotation towards the poles because of non-cylindrical rotation.

After subtraction of the radial component of the spatial velocity of each cluster as a whole ($\bar{V} = 232.6$ km/s for ω Cen; $\bar{V} = -19.5$ km/s for 47 Tuc), the rotational velocity fields are clearly displayed.

Fig. 2 shows the equatorial rotation curve of ω Cen whereas the non-cylindrical character of the rotation appears in Fig. 3. It is interesting to point out the structural resemblance between both clusters through the fact that the rotational velocity peaks in both cases between 3 and 4 core radii.

Velocity Dispersion

Contributions of rotation and integration along the line of sight having been eliminated, the velocity dispersion component due only to random motions was obtained, under the assumption of isotropy, in a few concentric shells: for ω Cen, Fig. 4 and for 47 Tuc, Fig. 5. These results show the same tendency in both clusters: a slow and regular increase of the velocity dispersion from the edge of the cluster towards the centre, with large values in the core.

In order to discuss these surprising results, it is worthwhile to recall that if Gunn and Griffin (1979) do not find this central increase in their study of M3 (NGC 5272), this is due to the fact

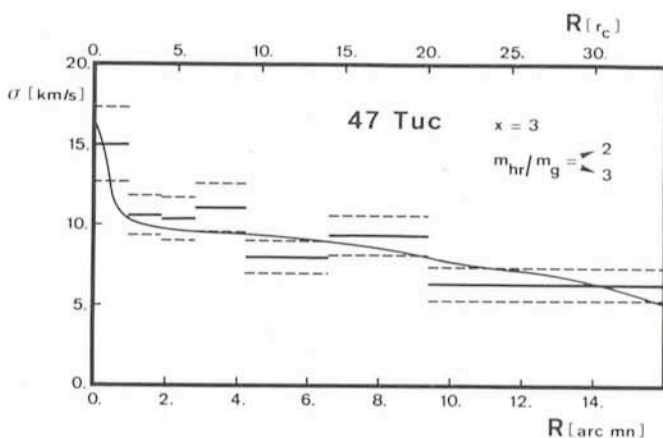


Fig. 5: 47 Tuc: observed velocity dispersion and model velocity dispersion (continuous line) computed with IMF exponent $x = 3$ and with $m_{hr}/m_g = 2$ and 3 (both cases give the same result).

Tentative Time-table of Council Sessions and Committee Meetings in 1985

November 12	Scientific Technical Committee
November 13-14	Finance Committee
December 11-12	Observing Programmes Committee
December 16	Committee of Council
December 17	Council

All meetings will take place at ESO in Garching.

that they did not take into account two very-high velocity member stars of this cluster. If these two stars situated in the core of M3 are added to the sample of stars, the central velocity dispersion increases and shows a value greater than those of regions immediately outside.

For ω Cen and 47 Tuc, the distributions of residual velocities in the different shells were investigated. They do not present any significant divergence from normal laws, nor do they have very high velocity stars. Hence the large central values of the velocity dispersions obtained in the centres of ω Cen and 47 Tuc are not due to a few stars with exceptional velocities.

The dynamical importance of binaries in the evolution of globular clusters is now well established; in particular, because of equipartition, heavy binaries should be concentrated in the core. Thus it would be possible to think that at least a part of the central increase of the velocity dispersion could be explained by the existence of orbital motions of binary stars. The twice measured stars in the cores of ω Cen and 47 Tuc do not seem to confirm this idea.

The relative importance of ordered and random motions are given by the ratio v_o/σ_o , where v_o^2 is the mass-weighted mean square rotation speed and σ_o^2 the mass-weighted mean square random velocity along the line of sight.

The results visible in Fig. 6 show that ω Cen and 47 Tuc are in close agreement with models of oblate axisymmetric systems

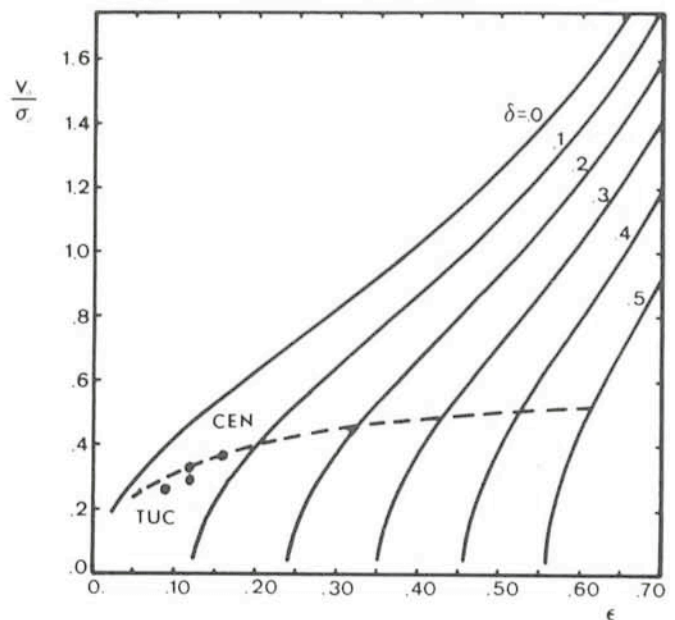


Fig. 6: Ratio v_o/σ_o of ordered to random motions in function of ellipticity ϵ and anisotropy δ . Due to the strong influence of the central part of the clusters, the present observed positions of ω Cen and 47 Tuc are in favour of a negligible anisotropy of the velocity distribution in the few central core radii.

study of M3). Radial velocities with an accuracy better than 1 km/s (about one tenth of typical internal motions in a globular cluster) are determined despite the relative faintness of these stars. This gives access, for example, to an understanding of the behaviour of the velocity dispersion as a function of the distance to the centre, to details of the field of rotation and to a search for spectroscopic binaries.

The latter, formed by dissipative two-body tidal capture or by three-body encounters, play an essential role in the dynamical evolution of a self-gravitating system. Depending on the formation mode, binaries can give up energy to passing stars, becoming more and more tightly bound. The energy made available may slow down or even reverse the collapse of the core.

Accurate Radial Velocities thanks to CORAVEL

Set up at the Cassegrain focus of the 1.5 m Danish telescope at La Silla, the CORAVEL photoelectric spectrometer provides high-quality radial velocities (Baranne et al. 1979, *Vistas in Astronomy*, **23**, 279).

The mean accuracy per measurement is 0.6 and 0.9 km/s for 47 Tuc and ω Cen respectively. More than 600 radial velocity measurements of stars, mainly between B mag 13 and 15, have been carried out through collaboration between observers from ESO, the Copenhagen, Marseilles and Geneva Observatories (Mayor et al, 1983, *Astron. Astrophys. Suppl.* **54**, 495).

The kinematical and dynamical description given below was obtained through the mean radial velocities of 298 member stars in ω Cen and 192 member stars in 47 Tuc. These stars are uniformly distributed from the centres to 9.3 core radii for ω Cen and to 30.5 for 47 Tuc.

King's concentration parameters $c = \log(r_t/r_c)$, logarithm of the ratio of the tidal radius r_t to the core radius r_c , for these two clusters underline their important differences of structure: ω Cen is a rather loose cluster with $c = 1.36$, $r_c = 2.4$ arcmin, $r_t = 55$ arcmin, whereas 47 Tuc shows a strongly condensed core with $c = 2.03$, $r_c = 0.47$ arcmin and $r_t = 50$ arcmin. This structural disparity involves immediate consequences on the observation of individual stars in the central regions: there is no problem of identification of stars in ω Cen even inside one core radius but for 47 Tuc the high central brightness saturates all the photographic plates. Nevertheless, since the acquisition of very central radial velocities is essential for determining the maximum of the rotation law as well as for obtaining the

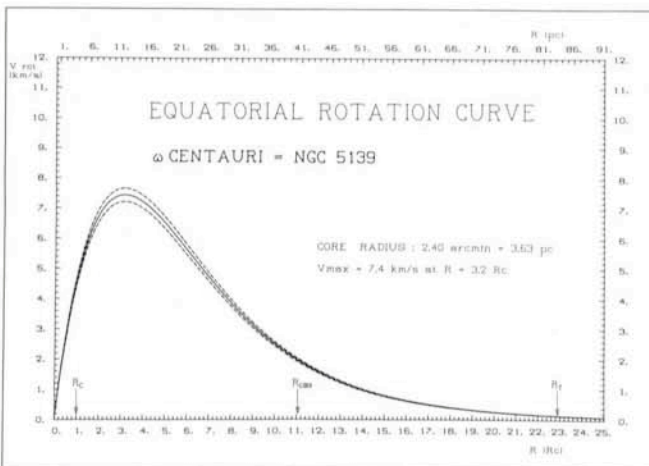


Fig. 2: Equatorial rotation curve of ω Cen deduced from radial velocities of 298 individual stars (under the hypothesis that the cluster is viewed equator-on).

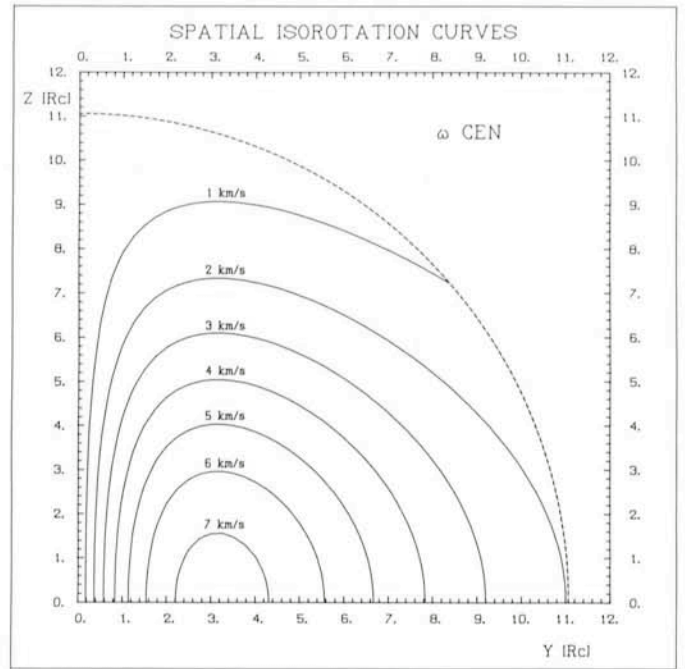


Fig. 3: Smoothed velocity field deduced from ω Cen radial velocity measurements: spatial isorotation curves drawn on a meridional plane containing the rotation axis of the cluster (under the hypothesis of an equator-on view of the cluster)

real central velocity dispersion, an IR plate of the nucleus of 47 Tuc (Lloyd Evans, 1974) was used to identify central stars. We were extremely lucky to discover that, by decreasing the gain of the TV monitor at the 1.5 m Danish telescope, the inner part of this cluster appeared very similar to the IR chart (Fig. 1), thus making the measurement of radial velocities of individual stars feasible.

Rotation

It is well known that the flattening of elliptical galaxies is not necessarily due only to rotation, the latter being generally too weak to explain the large observed ellipticities. An alternative to galaxian rotation seems to be an anisotropy of the velocity dispersion in triaxial ellipsoids or oblate spheroids. In the case of globular clusters, the problem looks different; we then observe the internal parts in which the relaxation time scale is relatively short. Thus, at least in the central parts where rotation is expected, velocity dispersion obtained through dynamical models of globular clusters appears nearly isotropic. Given the small mean ellipticities of these clusters, we may think that their flattening is due to rotation, the latter being generally weak and therefore detectable with difficulty. Even though the rotation of some globular clusters had already been detected (ω Cen by Harding, ROB, 1965; M13 by Gunn and Griffin [unpublished]; 47 Tuc by Mayor et al, 1984, *AA* **134**, 118), no detailed velocity field $V(r, z)$ was determined (distance r to the rotation axis and z to the equatorial plane).

The main characteristics of the velocity fields for the two clusters studied can be summarized as follows:

- (i) solid-body rotation in the nucleus
 ω Cen : $\Omega_c = 4.6 \text{ km s}^{-1} r_c^{-1} = 1.3 \cdot 10^{-6} \text{ y}^{-1}$
 47 Tuc : $\Omega_c = 2.7 \text{ km s}^{-1} r_c^{-1} = 4.9 \cdot 10^{-6} \text{ y}^{-1}$
- (ii) the maximum velocity V_{\max}
- (iii) the position of this maximum as a function of the radius
 ω Cen : $V_{\max} = 7.4 \text{ km s}^{-1}$ at $r = 3.2 r_c$
 47 Tuc : $V_{\max} = 4.6 \text{ km s}^{-1}$ at $r = 3.5 r_c$

with small ellipticity and slight anisotropy. The dashed line shows the trajectory followed by $[v_o(i)/\sigma_o, \epsilon_{app}(i)]$ when i decreases from 90° (equator on) while ϵ_{true} , the true ellipticity, and δ , the anisotropy parameter, are held constant. For both of these clusters results are given for $i = 90^\circ$ and 60° .

Masses and Mass-Luminosity Ratios

The simultaneous knowledge of the velocity dispersion $\sigma(r) = \sqrt{v^2(r)}$ (corrected for rotation) and of the normalized space density distribution $v(r) = \varrho(r)/\varrho(0)$ of a population of test particles (here the giant star population) moving in a spherical cluster allows, under the hypothesis of the velocity dispersion isotropy, to determine directly the total gravitational potential. In the same order of approximation, the weak rotation can here be neglected. It is then possible to deduce the total dynamical mass $M(r)$ inside the radius r of the cluster, via the following equation:

$$\frac{GM(r)}{r} = -\sigma^2 \left[\frac{d \ln v}{d \ln r} + \frac{d \ln \sigma^2}{d \ln r} + 2\beta \right]$$

where $\beta = 0$ for the systems with isotropic velocity dispersion. However, in globular cluster cores, the limited number of stars for which the radial velocity can be determined does not allow a sufficiently precise determination of $\sigma(r)$ in order to give the variations of $d \ln \sigma^2 / d \ln r$ in the central regions. The same lack of accuracy affects the knowledge of $d \ln v / d \ln r$.

If we suppose on the one hand that the cluster consists of several sub-populations with different individual masses and, on the other hand, equipartition of the energy, the shape of the function $\sigma(r)$ can be deduced. The radial variation of $\sigma(r)$ depends on the percentage of heavy remnants (degenerated stars with masses larger than the mass of the test particles), on the mass function of the main sequence and on the total mass of the cluster. Certainly, such an approach would benefit from

a better defined luminosity function of the lower part of the main sequence (an expected task for the Space Telescope).

The observed dependence of the velocity dispersion with the distance to the centre implies, for any chosen IMF compatible with the total luminosity constraint, the presence of heavy remnants in the core of ω Cen. These objects, with individual masses larger than the giant stars by a factor of 2 or 3, represent about 7 per cent of the total mass of the cluster. Due to mass segregation, the ratio of the density of heavy remnants to the total density is very large in the nucleus (for ω Cen this ratio can be of about 35 %).

On the other hand, the radial velocity dispersion of 47 Tuc seems to require only 1 to 3 per cent of heavy remnants in comparison to the total mass.

For these two globular clusters, the total masses derived from our analysis are:

$$\begin{aligned} \text{total mass of } \omega \text{ Cen} &\approx 2.9 \cdot 10^6 \text{ solar masses} \\ \text{total mass of 47 Tuc} &\approx 1.3 \cdot 10^6 \text{ solar masses} \end{aligned}$$

which implies mass-to-luminosity ratios between 2 and 3.

The sub-population with individual masses between 1.5 and 2 solar masses consists most probably of the remnants issued from the evolution of the most massive stars of the globular clusters initial mass function. But part of this sub-population could also be binaries. The observed radial distribution of X-ray sources in globular clusters presents a notable concentration towards the core, in agreement with the dynamical segregation of individual masses of about 1.5 solar masses.

If the fact that the high stellar densities expected in collapsed cores are favourable to binary formation and if the detected X-ray sources are binaries, it would be important to recall the total absence (or at least large deficiency) of spectroscopic binaries in globular clusters. Continuing observations of stellar radial velocities, particularly in the cores of globular clusters, should create some new constraints regarding their dynamics.

R136a and the Central Object in the Giant HII Region NGC 3603 Resolved by Holographic Speckle Interferometry

G. Weigelt, G. Baier and R. Ladebeck, *Physikalisches Institut Erlangen*

R136 (HD 38268) is the mysterious central object of the 30 Doradus nebula in the Large Magellanic Cloud (Walborn, 1973). R136 consists of the bright component R136a and the fainter components R136b and R136c (Feitzinger et al., 1980). There exist mainly two opinions about the nature of R136a: that it is either a supermassive object with $M \sim 1,000$ to $3,000 M_\odot$ (Schmidt-Kaler and Feitzinger, 1981; Cassinelli et al., 1981) or that it is a dense star cluster consisting of O and WR stars (Moffat and Seggewiss, 1983; Melnick, 1983).

Speckle interferometry observations (Labeyrie, 1970) of R136a have been reported by Weigelt (1981), Meaburn et al. (1982) and Weigelt (1984). Our speckle measurements of the $0''.5$ component are in agreement with visual observations made by Innes (1927) and Worley (1984) as well as with photographic measurements by Chu et al. (1984) and by Walker and O'Donoghue (1985).

In this paper we show the first diffraction-limited true image of R136a (Fig. 2). This image shows that R136a is a dense star cluster consisting of at least 8 stars. It was possible to reconstruct a true image of R136 a1 to a8 by using R136b (separation $\sim 2''.1$) and R136c (separation $\sim 3''.3$) as deconvolution keys (holographic speckle interferometry). The

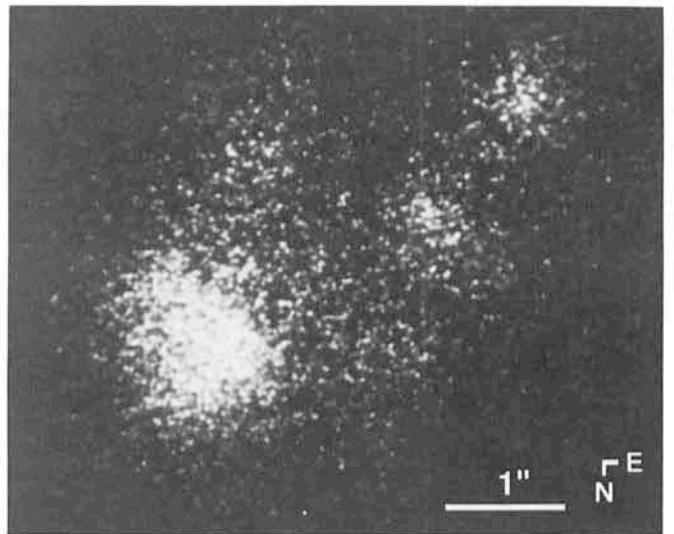


Fig. 1: Speckle interferogram of R136. The brightest speckle cloud is R136a, the other speckle clouds are R136b to e (filter RG 610, exposure time 1/15 sec).

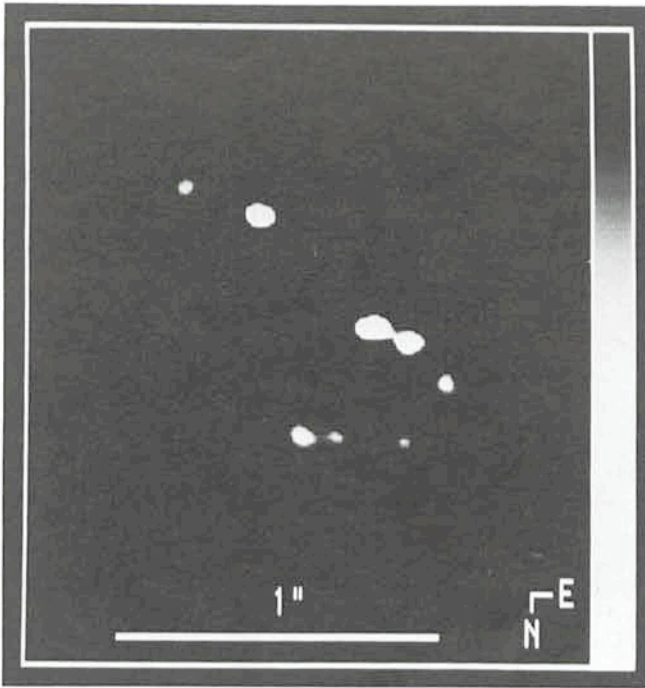


Fig. 2: Diffraction-limited image of R136 a1 to a8 reconstructed from 4,000 speckle interferograms (Danish 1.5 m telescope, filter RG 610). The dominating stars are R136 a1, R136 a2 (separation = $0''.10$) and R136 a3 (separation = $0''.48$). The double star R136 a1-a2 is the close eastern double object. The four fainter objects are R136 a4 to a8.

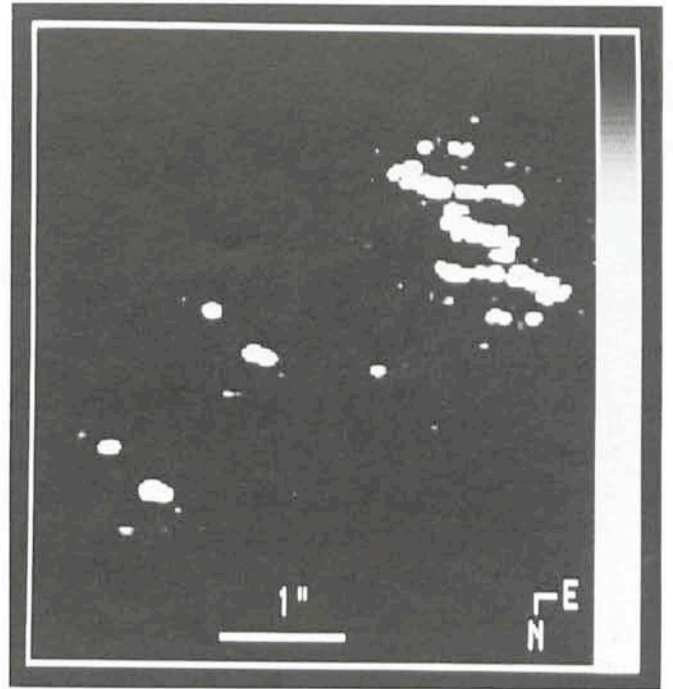


Fig. 4: One half of the autocorrelation of R136abc. It can easily be seen that the autocorrelation contains two true images of R136a caused by the holographic reference stars R136b and R136c.

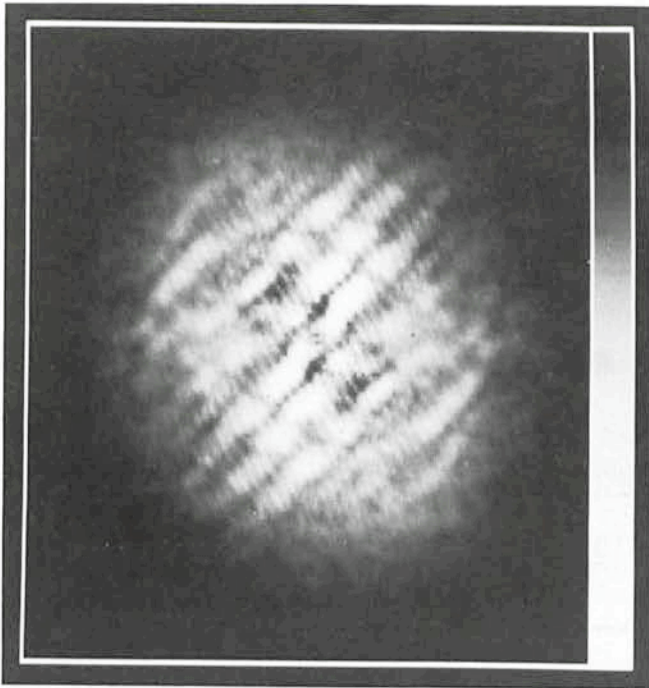


Fig. 3: Power spectrum of R136abc (= hologram of R136a).

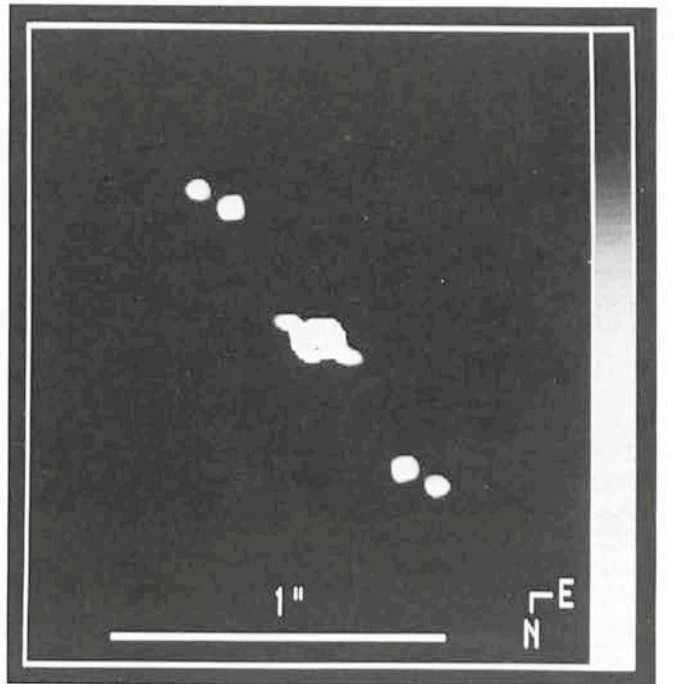


Fig. 5: Autocorrelation of R136 a1-a2-a3 reconstructed from data recorded with the 2.2 m telescope (filter $\lambda_0 = 610\text{ nm}/\Delta\lambda = 120\text{ nm}$). The off-axis double dot is a true image of R136a1-a2 (separation = $0''.10$).

dominating objects in R136a are the three bright stars R136 a1, a2 and a3 which have almost identical magnitudes. The separations of a1-a2 and a1-a3 are $0''.10$ and $0''.48$, respectively. The reconstructed image has a resolution of $0''.09$.

Figs. 1 to 5 show some of our speckle results. Fig. 1 is one of the speckle interferograms of R136abc recorded with the Danish 1.5 m telescope (Schott filter RG 610, S20-cathode with extended red response, exposure time 1/15 sec).

Fig. 2 is the high-resolution image of R136 a1 to a8 reconstructed digitally from 4,000 speckle interferograms (Danish 1.5 m telescope, filter RG 610).

Fig. 3 is the object power spectrum of R136abc or the hologram of R136 a1 to a8.

Fig. 4 shows one half of the autocorrelation of R136abc. The autocorrelation contains two true images of R136a which are caused by the reference stars R136b and R136c. The useful-

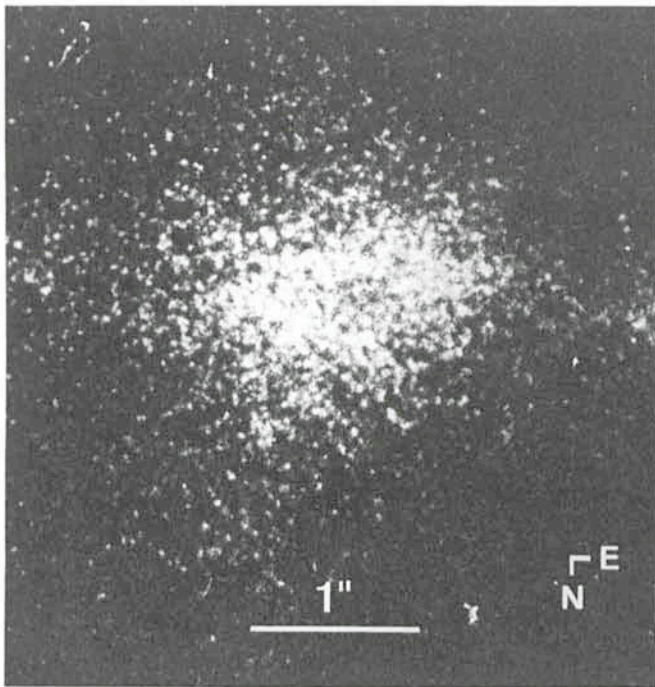


Fig. 6: Speckle interferogram of HD 97950 AB.

ness of such reference stars has been discussed by Liu and Lohmann (1973) and Weigelt (1978) in more detail.

Fig. 5 shows the autocorrelation of R136 a1–a2–a3 reconstructed from 4,000 speckle interferograms recorded with the 2.2 m telescope (filter $\lambda_0 = 610 \text{ nm}/\Delta\lambda = 120 \text{ nm}$). This autocorrelation has higher resolution than the 1.5 m autocorrelation. Therefore the a1–a2 image (= off-axis double peak) is better resolved. More details about our R136a observations are described in a paper submitted to *Astronomy and Astrophysics* (Weigelt and Baier, 1985).

Figs. 6 and 7 show one speckle interferogram and the high-resolution autocorrelation of HD 97950 AB in the giant HII region NGC 3603. We have investigated this object since it has been discussed in various papers that it may be of similar nature as R136a (Moffat and Seggewiss, 1984). The autocorrelation shows that HD 97950 AB is a star cluster consisting of 4 stars. We found that the component A is a triple star and B is a single star (see Baier et al., 1985 for more details). Since B is a single star, the three peaks on the extreme left of the autocorrelation are a true image of HD 97950 A1–A2–A3.

References

- Baier, G., Ladebeck, R., Weigelt, G.: 1985, Speckle interferometry of the central object in the giant HII region NGC 3603, submitted to *Astron. Astrophys.*
- Cassinelli, J.P., Mathis, J.C., Savage, B.D.: 1981, *Science* **212**, 1497.
- Chu, Y.-H., Cassinelli, J.P., Wolfire, M.G.: 1984, *Astrophys. J.*, **283**, 560.
- Feitzinger, J.V., Schlosser, W., Schmidt-Kaler, Th., Winkler, Chr.: 1980, *Astron. Astrophys.* **84**, 50.
- Innes, R.T.A.: 1927, Southern double star catalog, Unions Obs., Johannesburg.
- Labeyrie, A.: 1970, *Astron. Astrophys.* **6**, 85.
- Liu, C.Y.C., Lohmann, A.W.: 1973, *Optics Commun.* **8**, 372.
- Meaburn, J., Hebden, J.C., Mogan, B.L., Vine, H.: 1982, *Mon. Not. R. Astron. Soc.* **200**, 1 p.
- Melnick, J.: 1983, *The Messenger* **32**, 11.
- Moffat, A.F.J., Seggewiss, W.: 1983, *Astron. Astrophys.* **125**, 83.
- Schmidt-Kaler, Th., Feitzinger, J.V.: 1981, in: *The Most Massive Stars*, Proc. ESO workshop, eds. S. D'Odorico, D. Baade and K. Kjär, Garching, Europ. Southern Obs., p. 105.
- Walborn, N.R.: 1973, *Astrophys. J.* **182**, L21.

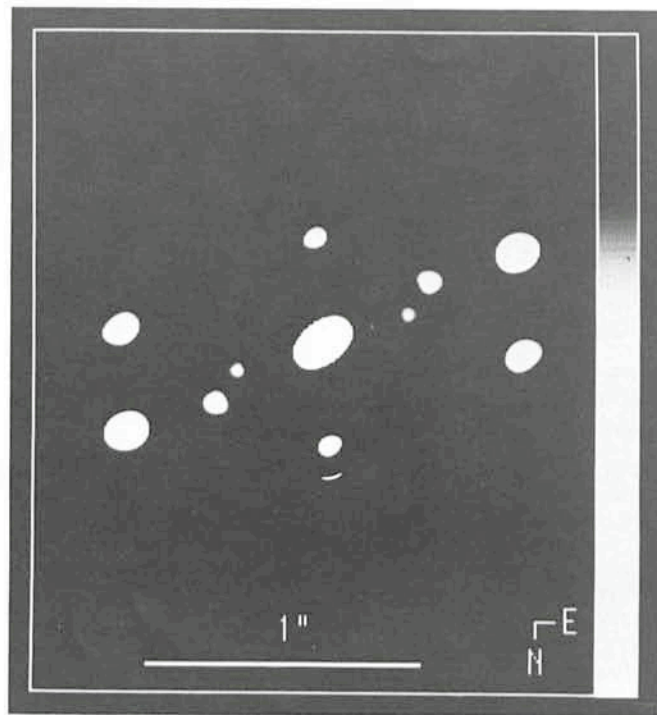


Fig. 7: High-resolution autocorrelation of HD 97950 A1–A2–A3–B. The three dots on the extreme left are a diffraction-limited image of HD 97950 A1–A2–A3.

- Walker, A.R., O'Donoghue, D.E.: R136: Multiple or Monster? in press.
- Weigelt, G.: 1978, *Appl. Opt.* **17**, 2660.
- Weigelt, G.: 1981, in Proc. of the ESO Conf. on "Scientific Importance of High Angular Resolution at IR and Optical Wavelengths", eds. M.H. Ulrich and K. Kjär, Garching, March 1981, p. 95.
- Weigelt, G.: 1984, in Proc. of the IAU Colloquium No. 79: "Very Large Telescopes, their Instrumentation and Programs, April 9–12, ESO, Garching, p. 337.
- Weigelt, G., Baier, G.: 1985, R136a in the 30 Dor nebula resolved by holographic speckle interferometry, submitted to *Astron. Astrophys.*
- Worley, C.E.: 1984, *Astrophys. J.* **278**, L109.

Access to IRAS Data in ESO Member Countries

Several of the official IRAS products have now been released to the general astronomical community, others will follow in the near future.

Already released are:

- Point Source Catalog, containing 250,000 point sources detected in at least one of the IRAS bands (12, 25, 60 and 100 μ). Print, microfiche and tape versions (2 tapes, 1,600 BPI).
- Working Survey Data Base, containing the observation history of objects in the point source catalog. Print and tape versions (2 tapes, 6,250 BPI).
- Skyflux Maps, in $16^\circ \times 16^\circ$ overlapping fields in each of the IRAS bands. These maps are preliminary, as they are based only on the third and last IRAS sky coverage (HCON3). Photographic and tape versions (188 images and 20 tapes, 6,250 BPI).
- Catalog of Low Resolution ($\lambda/\Delta\lambda = 20$) Spectra of $\approx 5,000$ sources (LRS Catalog), mainly late-type stars. Tape versions only; print version will appear in *A & A Supplements* in 1985 (1 tape, 1,600 BPI). Soon to be released will be:
- Catalog of variable sources.
- Skyflux maps containing data from all IRAS sky coverages (HCON's 1, 2 and 3 [revised]).

– Catalog of Small Extended Sources.

Several other, more primitive products, various IRAS databases, including the LRS database, and large-scale maps (Spline I, Spline II) will remain at the designated IRAS Centers.

These Centers are:

Netherlands: Leiden, Groningen, and Amsterdam Astronomical Institutes;

UK: Rutherford Appleton Labs, Chilton;

USA: SDAS Center, now at JPL, Pasadena, to be moved to Caltech summer 1985.

All three Dutch data centers possess the officially released products as well as additional handling software. There is some specialization, however:

Amsterdam

Pannekoek Institute: All official products plus Astronomical Catalogs for cross-referencing with IRAS PS catalog.

Groningen

Ruimteonderzoek: All official products plus CPC Spline I, II Database, Survey Database (PASS), Colour Display (AO Deep Sky Grids).

Leiden

Sterrewacht: All official products plus LRS Database. (Spline I, II) Survey Database (CCDD), Plate Scanning Device plus software, Colour Display, AO Deep Sky Grids.

All officially released products will also reside at the Stellar Data Centre, Strasbourg.

European astronomers wishing to make use of IRAS data are kindly requested to take note of the following:

- Copies of IRAS official products as mentioned above should be requested from the Stellar Data Center, Centre de Données Stellaires, Observatoire de Strasbourg, 11, Rue de l'Université, F-67000 Strasbourg. Dutch centers will not, as a rule, supply copies; requests will be passed on to Strasbourg.
- Under certain conditions, European astronomers will have access to databases and software (not officially released) at one of the Dutch data centers.
- Due to manpower restrictions, only limited service is available, so that prospective users will generally be required to come to the Netherlands in person.
- Small programs will entail a stay in the Netherlands varying from a minimum of two days to one or two weeks. Manuals and advising personnel are available for this type of program.
- Larger programs, making extensive use of IRAS products, databases and software, will require a longer stay and more extensive interaction with Dutch staff, possibly in the form of a full collaboration.
- Prospective European users of the Dutch facilities are in all cases requested to contact:

Chairman Dutch IRAS Steering Group
Dr. H. J. Habing
Sterrewacht Leiden
Wassenaarseweg 78
2300 RA Leiden

Nova-like Objects and Dwarf Novae During Outburst – A Comparative Study

W.F. Wargau, University of South Africa

General Remarks on Cataclysmic Variables

The Model

Novae, recurrent novae, dwarf novae and nova-like objects form subgroups of a class of objects well known as cataclysmic variables. Detailed photometric and spectroscopic work during the past thirty years has shown that all of them are interacting double stars. The primary component represents a massive white dwarf—the mass average lies at about one solar mass, and much of the observed dispersion is due to uncertainties in the reduction procedures—in contrast with field white dwarfs which possess an average mass at about 0.65 solar masses (Weidemann, 1968). The secondary component comprises a late-type main-sequence dwarf with spectral type K to M which fills its critical Roche volume, and spilling hydrogen-rich material via the Lagrangian point L1 to the highly evolved primary. Due to conservation of angular momentum the mass stream does not immediately impact the primary but leads to the formation of a quasi-stable accretion disk. At the impact zone of transferred material and particles in the outer disk region, an area of shocked gas—the so-called hot spot—is produced. By exchange of angular momentum, disk material spirals slowly inward, and is finally accreted onto the primary component. In fact, it is this interplay of mass transfer and accretion processes which is responsible for most of the peculiar behaviour observed in this class of objects.

The Outburst Activity

The principal difference between cataclysmic variables is linked with their outburst activity. Novae reveal less frequent

outbursts with a quiescent phase of about 10^4 to 10^5 years between explosions, while recurrent novae erupt on the average between 10 and a few hundred years. The outburst amplitude is 7^m to 14^m , and the mean energy radiated per single eruption amounts to $\leq 10^{45}$ ergs. It is now well established that the nova explosions result from unstable thermonuclear burning of hydrogen-rich material, accreted and accumulated onto the surface of the otherwise hydrogen-exhausted white dwarf. The dwarf nova eruptions occur more frequently in intervals between 10 days and several years, their amplitudes range between 2^m to 6^m and the total energy released per outburst is of the order of 10^{38} to 10^{39} ergs. Due to recent theoretical models (Papaloizou et al., 1983) recurrent instabilities in the accretion disk itself—caused by different viscosity values—are responsible for the explosions. At low density the viscosity is low, and the material is stored in a ring. As soon as the density in this ring reaches a critical value, the viscosity increases rapidly and the ring expands into a disk with a great portion of its mass accreting onto the white dwarf. This conversion of gravitational potential energy of the ring into radiation causes the observed dwarf nova outburst. According to their outburst behaviour, the dwarf novae are subdivided into U Gem, Z Cam and SU UMa-type stars. U Gem-type stars exhibit typical dwarf nova eruptions: the rise to maximum brightness takes a shorter time than the recovery from maximum to quiescence. On the average an eruption lasts for several days. Z Cam-type stars are characterized by a brightness "standstill": after a regular outburst it sometimes happens that the brightness remains about one magnitude below peak brightness for an indefinite period of time (it can last hours to even years). SU UMa-type stars undergo, besides regular outbursts, additional superoutbursts which show a larger outburst amplitude (up to several magnitudes), and

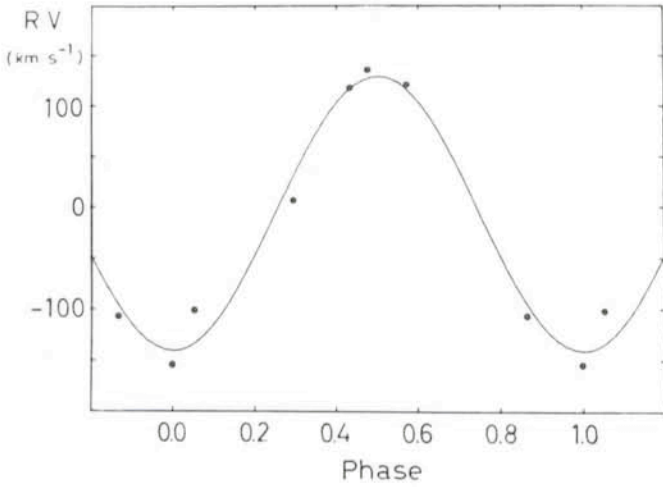


Fig. 1: Radial velocity curve of CPD-48°1577. The orbital phase corresponds to the ephemeris $JD\ 2445334.552 + 0.187\ E\ \text{day}$. For further explanations see text.

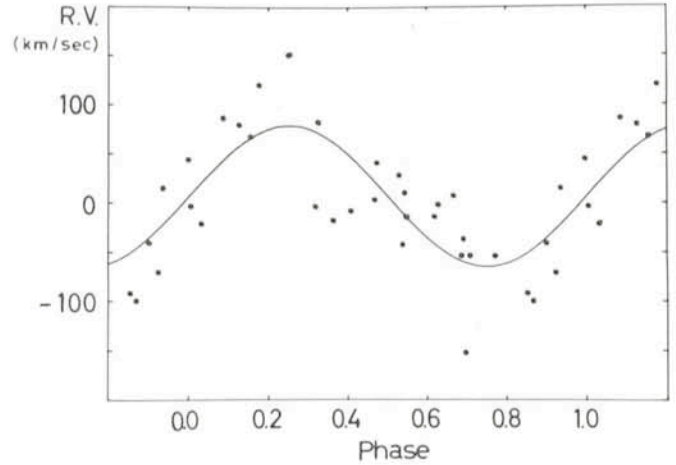


Fig. 2: Radial velocity curve of HL CMA. The orbital phase corresponds to the ephemeris $JD\ 2445329.560 + 0.2145\ E\ \text{day}$. For further explanations see text.

whose durations are 3 to 4 times longer than that of a normal eruption. The nova-like variables show no spectacular explosion but their photometric and spectroscopic activities are closely related to cataclysmic systems.

Dwarf Novae—Nova-like Objects

Already in 1974, it has been suggested by B. Warner and W.G. van Citters that some nova-like variables, e.g., TT Ari, UX UMa, BD-7°3007, CD-42°14462, Feige 24 and VY Scl, could be Z Cam-type variables permanently stuck in a standstill phase. The authors concluded this from the similarity between dwarf nova spectra taken during outburst and nova-like spectra. Indeed, successful UV spectroscopy of TT Arietis with the IUE satellite during July 1979 and January 1981 has led to a reclassification as a Z Cam-type variable (Krautter et al., 1981; Wargau et al., 1982). In November 1980 the system showed a sudden drop from its mean brightness level of 11^m to $14^m.5$. The following month, December 1980, TT Ari rebrightened again, and returned to an intermediate brightness level of $11^m.8$ in January 1981. However, inspection of photographic material back to 1905 show no indication of a regular outburst. Additionally, the time to reach the intermediate maximum brightness took longer than usual. During 1981 and 1982 the brightness faded down to below 16^m , where the system has remained up to now. Possibly, this indicates dramatic changes in the transfer and accretion processes which undoubtedly influence the evolution of TT Arietis. Certainly, more photometric and spectroscopic work has to be done on this peculiar system before a final classification can be made.

The Observation Programme

During the past years a long-term observing project of cataclysmic variables—with emphasis on dwarf novae and nova-like objects—has been established at ESO. Amongst the programme stars in particular two systems turned out to be most exciting: the nova-like variable CPD-48°1577 and the peculiar dwarf nova HL CMA.

CPD-48°1577—also catalogued as CD-48°3636, SS 1024 and KS 155—has been discovered recently as a cataclysmic variable by R. F. Garrison et al. (1982). The authors carried out a MK spectral classification survey of southern OB stars, and discovered some unusual characteristics in this system: the UBV colours are not typical of an OB star,

continuous brightness fluctuations—so-called “flickering”—of the order of $0^m.1$ occur on a time scale of minutes, and the hydrogen and helium I and II absorption lines appear extremely weak and broad. Spectroscopic observations in the ultraviolet with the IUE satellite by H. Böhnhardt et al. (1982) revealed CPD-48°1577 as a nova-like object or a dwarf nova at outburst phase. Due to its remarkable brightness (in respect with cataclysmic variables) of $9^m.4$, CPD-48°1577 is one of the brightest cataclysmic systems.

HL CMA represents the optical counterpart of the variable, hard X-ray source 1E0643.0-1648 (Chlebowski et al., 1981). Its long-term optical variability as well as its photometric behaviour (flickering activity) makes this system a typical member of the dwarf nova class. HL CMA exhibits a quite short mean outburst cycle of 15 days.

The corresponding spectroscopic observations were carried out in December/January 1982/1983 with the ESO 1.5 m telescope equipped with the Boller & Chivens Cassegrain spectrograph and an Image Dissector Scanner (Wargau et al., 1983a, 1983b). The spectra covering a wavelength range from $4080\ \text{\AA}$ to $5260\ \text{\AA}$ have a dispersion of $59\ \text{\AA}/\text{mm}$. Additional infrared photometry in the filters J ($1.25\ \mu\text{m}$), H ($1.65\ \mu\text{m}$), K ($2.2\ \mu\text{m}$) and L ($3.4\ \mu\text{m}$) with the ESO 1 m telescope using an InSb photometer was obtained in January/February 1983 (Wargau et al., 1984). The integration time of a single filter measurement was 20 seconds, and in the reduction procedure a set of JHKL data were connected together.

The Comparative Study

The Orbital Periods

For CPD-48°1577 we obtained 5 spectra continuously over a time interval of several hours. In the case of HL CMA, 31 spectra could be taken in three consecutive nights. The orbital periods have been derived by the radial velocity measurements of the hydrogen emission lines. The corresponding radial velocity curves of CPD-48°1577 and HL CMA are displayed in Figs. 1 and 2, respectively. The dots represent the velocities of the hydrogen lines; the solid curve is a least squares sine-fit to the data. While for HL CMA the orbital period is quite well determined, the data for CPD-48°1577 are rather poor. Therefore, the latter period can only be considered as preliminary so far. The derived orbital periods are 4^h29^m and 5^h09^m for CPD-48°1577 and HL CMA, respectively.

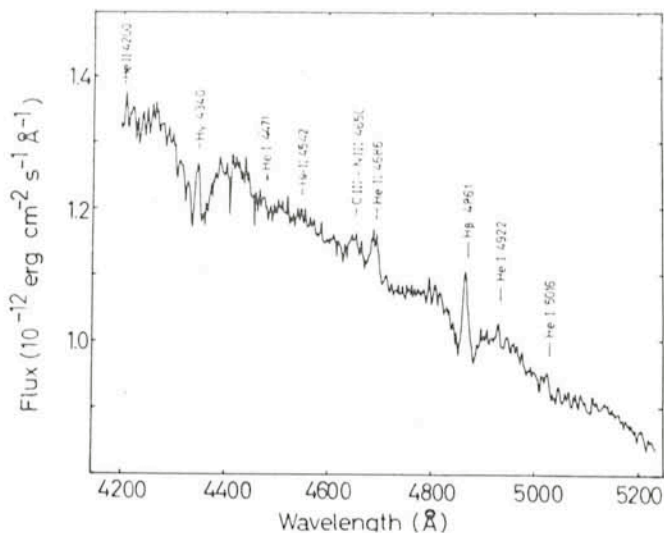


Fig. 3: Spectrum of CPD-48°1577. The spectrum represents a mean of five individual IDS spectra taken on December 30, 1982. The ordinate is given in absolute flux units which were obtained by using absolutely calibrated ESO standard stars. A correction for interstellar extinction has not been applied.

Our orbital period for HL CMa is close to the longer period suggested previously by Hutchings et al. (1981).

The orbital periods of cataclysmic variables are generally in the range from 80 minutes to 10 hours. By an inspection of all the available orbital periods one finds a clear gap in the 2 to 3 hour range. All objects with periods $P \geq 3$ hours are either novae, nova-like systems, U Gem or Z Cam subtypes; those with periods $P \leq 2$ hours are all SU UMa subtypes. The AM Her stars (a subtype of nova-like variables) are the only systems that bridge the gap. Our derived orbital periods fit quite well into this picture.

The Spectral Features and Continuum Distributions

For other reasons, the collected spectra seemed to be rather exciting: in our first observing night the dwarf nova HL

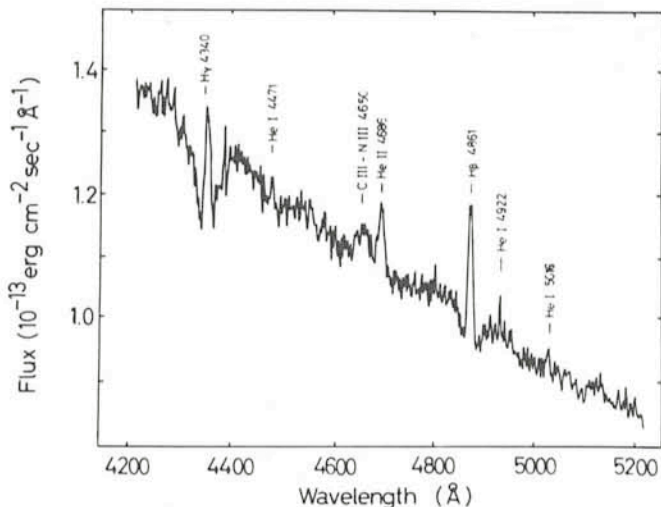


Fig. 4: Outburst Spectrum of HL CMa. The spectrum represents a mean of eight individual IDS spectra taken on December 26, 1982. The ordinate is given in absolute flux units which were obtained by using absolutely calibrated ESO standard stars. A correction for interstellar extinction has not been applied.

CMa was at the final ascent to peak brightness, remained in its outburst stage in the subsequent nights, and started to decline during the last observing night. The prospects are a direct comparison of an erupting dwarf nova and nova-like system. Figs. 3 and 4 show the spectra of CPD-48°1577 and HL CMa, respectively. Apart from the fact that the flux level in the nova-like system is a factor of 10 higher, the spectra reveal striking similarities: a relatively strong blue continuum is superimposed by broad hydrogen (Balmer) absorption troughs which are partly filled in by moderately strong emission components. Helium II (4686 Å), Helium I (4922 Å and 5016 Å) and Carbon III–Nitrogen III (4650 Å) lines are present in emission. Even the structure of the emission line profiles bear a strong resemblance: up to four different emission peaks can be distinguished. Figs. 5 and 6 show tracings of the hydrogen profiles arranged in respect with the orbital phase for CPD-48°1577 and HL CMa, respectively. In particular, no systematic variations with the orbital revolution can be inferred. In fact, those profiles reflect a complex velocity structure of the emitting region which can be attributed to the velocity structure in the accretion disk itself.

According to the cataclysmic variable model the wings of the absorption troughs should be generated by fast rotating particles in the innermost regions of the accretion disk in the vicinity of the white dwarf, while the emission lines reflect the motion of the particles in the outer disk regions. We investigated the involved velocities and found that the velocities reflected by the wings are about 2,200 km/sec and 4,000 km/sec, and the velocities derived at the half width at half maximum of the emissions are about 400 km/sec and 550 km/sec for CPD-48°1577 and HL CMa, respectively. In each case the velocities are corrected for the orbital inclination of the corresponding system. Also, the widths of the Helium II (4686 Å) line reveal quite similar results for both systems: the attributed velocities are some 30% larger than those of the hydrogen lines, indicating that they originate in hotter inner areas of the accretion disk.

The Infrared Observations

During our observing period, the infrared colours of CPD-48°1577 remained essentially constant. Furthermore, we checked a possible dependence of the infrared brightness on the orbital phase but were not able to find any dips or humps in the light curves. Actually the data show a large amount of scattering which could well overshadow small occultation or eclipse effects. The mean infrared colours are similar to those of other nova-like systems. On the other side the corresponding colours of dwarf novae at quiescence are on the average considerably redder. This might be due to different infrared contributions by the accretion disks and/or the late-type companion in dwarf novae and nova-like systems.

Conclusion

From our spectroscopic results it is quite obvious that CPD-48°1577 and HL CMa (at outburst stage) are closely related systems—in respect to the line features, the line profile structure and the continuum shape. So we might well conclude that the nova-like system CPD-48°1577 is a further candidate which is stuck in a permanent outburst stage—a dwarf nova of Z Cam subtype.

However, before a final decision can be drawn, a few “irregularities” have to be taken into consideration. First of all, the long-term variability—as derived from Bamberg sky-survey plates recorded between December 1963 and January 1973—shows no evidence for a quiescence stage or a pre-

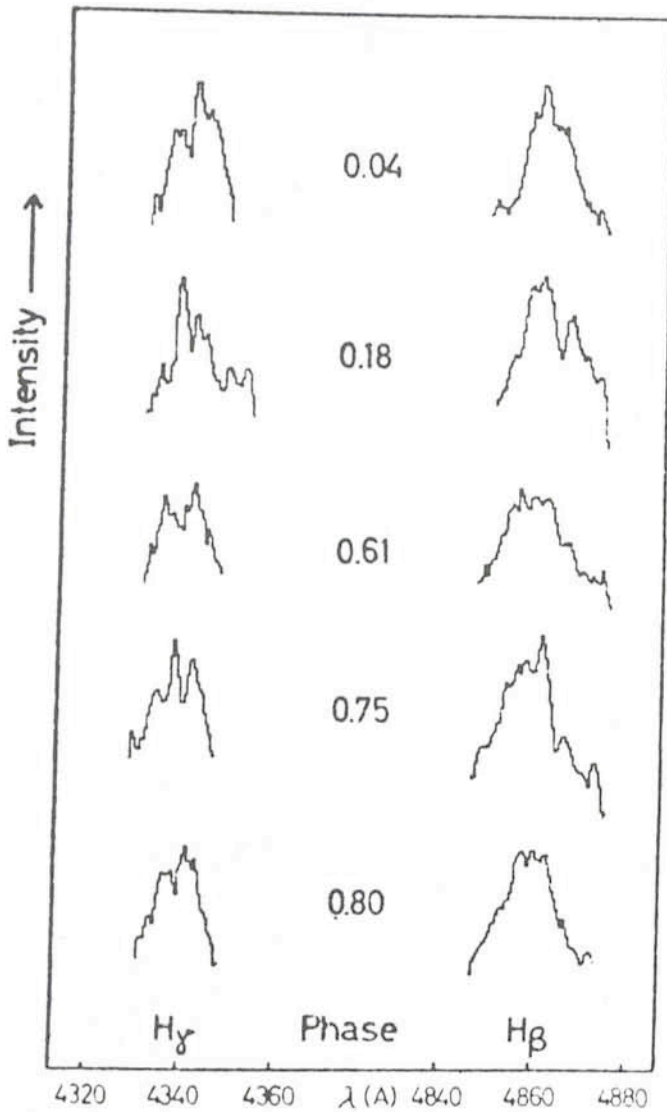


Fig. 5: Emission line profiles ($H\gamma$ and $H\beta$) of CPD-48°1577. The profile tracings are arranged according to the orbital phase. The ordinate is given in relative intensities.

ceding eruption. It may be that the time interval of the sky-survey plates is too short to allow for a definite statement. Also some spectral characteristics of HL CMA, as well as CPD-48°1577, appear more typical for ex-novae, e.g. the presence of the carbon III – nitrogen III (4650 Å) blend. Did CPD-48°1577 undergo an unrecorded classical nova outburst? In that case CPD-48°1577 would be one of the brightest known ex-novae. HL CMA at quiescence shows some evidence for a magnetic field of intermediate strength which, indeed, is not a

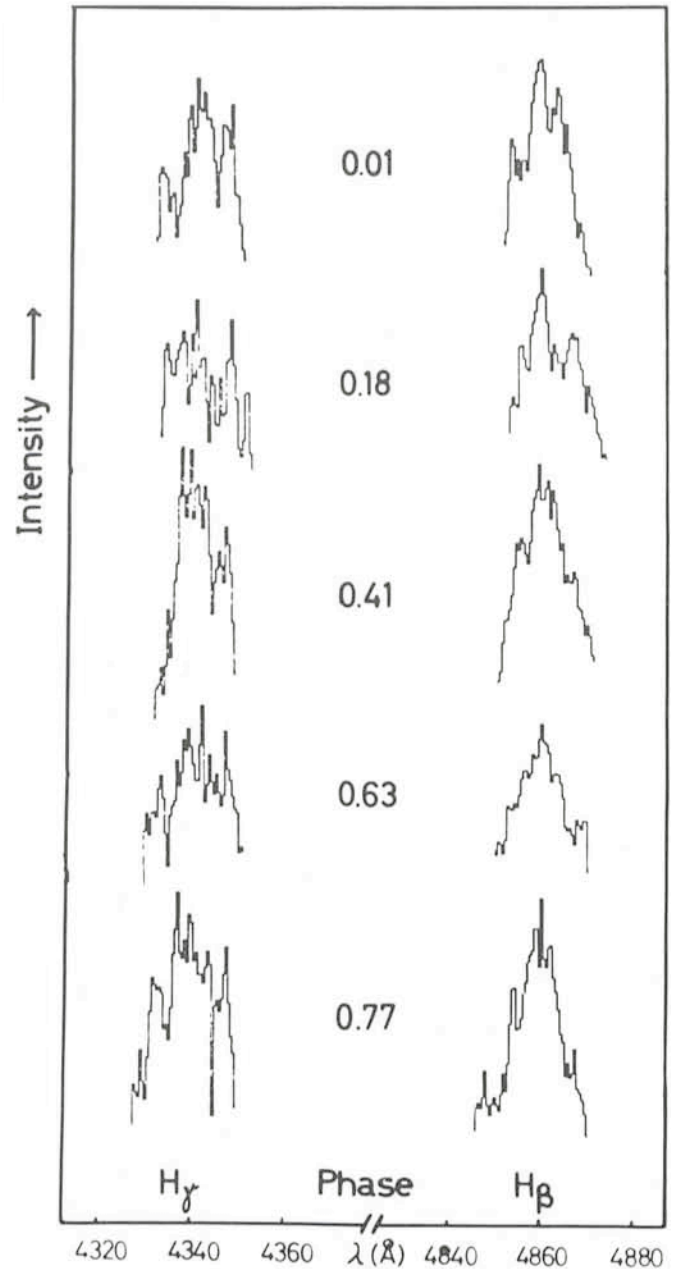


Fig. 6: Emission line profiles ($H\gamma$ and $H\beta$) of HL CMA. The profile tracings are arranged according to the orbital phase. The ordinate is given in relative intensities.

common dwarf nova feature; although its photometric appearance is typical for this group of stars.

In view of its brightness of $9^m.4$, CPD-48°1577 could become one of the most observed cataclysmic variables in the future. Professional astronomers, as well as amateurs, might find this system prolific for extended astronomical studies.

The Proceedings of the ESO Workshop on

The Virgo Cluster of Galaxies

which took place in Garching from 4 to 7 September 1984, have meanwhile been published. The price for the 477-page volume is DM 50.– (US\$ 18.–) and has to be prepaid.

If you wish to receive the Proceedings, please send your cheque to ESO, Financial Services, Karl-Schwarzschild-Str. 2, D-8046 Garching b. München, or transfer the amount to the ESO bank account No. 2102002 with Commerzbank München.

References

- Bönnhardt, H., Drechsel, H., Rahe, J., Wargau, W., Klare, G., Stahl, O., Wolf, B., Krautter, J.: 1982, IAU Circular No. 3749.
- Chlebowski, T., Halpern, J.P., Steiner, J.E.: 1981 *Astrophys. J.* **247**, L35.
- Garrison, R.F., Hiltner, W.A., Schild, R.E.: 1982, IAU Circular No. 3730.
- Hutchings, J.B., Cowley, A.P., Crampton, D., Williams, G.: 1981, *Publ. Astron. Soc. Pacific* **93**, 741.
- Krautter, J., Klare, G., Wolf, B., Wargau, W., Drechsel, H., Rahe, J., Vogt, N.: 1981, *Astron. Astrophys.* **98**, 27.

Papaloizou, J., Faulkner, J., Lin, D.N.C.: 1983, *Mon. Not. Royal Astron. Soc.* **205**, 487.
 Wargau, W., Drechsel, H., Rahe, J., Vogt, N.: 1982, *Astron. Astrophys.* **110**, 281.
 Wargau, W., Drechsel, H., Rahe, J., Bruch, A.: 1983a, *Mon. Not. Royal Astron. Soc.* **204**, 35p.

Wargau, W., Bruch, A., Drechsel, H., Rahe, J.: 1983b, *Astron. Astrophys.* **125**, L1.
 Wargau, W., Bruch, A., Drechsel, H., Rahe, J., Schoembs, R.: 1984, *Astrophys. Space Sci.* **99**, 145.
 Warner, B., van Citters, G.W.: 1974, *Observatory* **94**, 116.
 Weidemann, V.: 1968, *Ann. Rev. Astr. Astrophys.* **6**, 351.

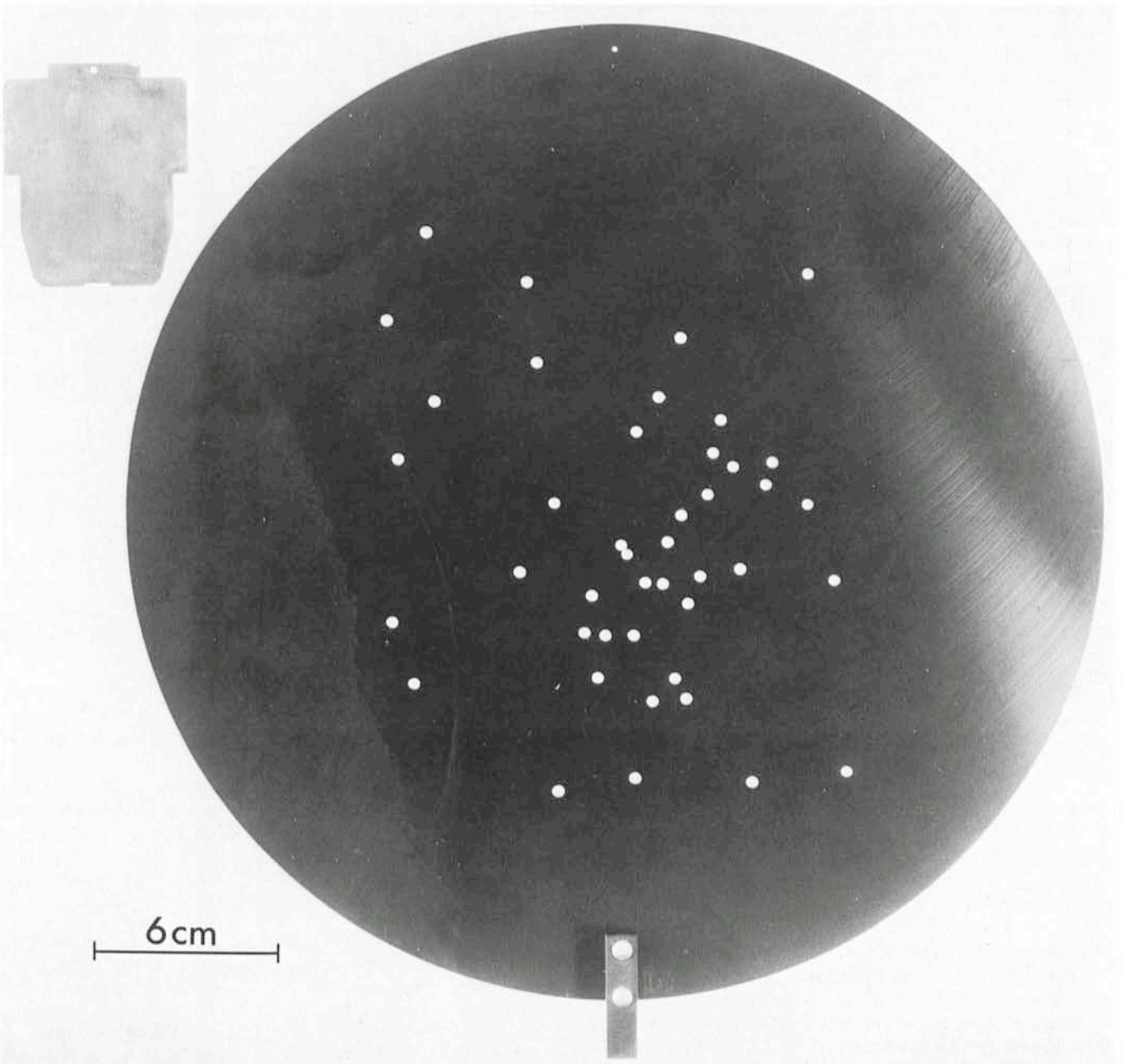
Two Multi-Object Spectroscopic Options at the ESO 3.6 m Telescope

In March, two instruments to obtain the spectra of several objects in a field in a single exposure were successfully tested at La Silla.

An improved version of OPTOPUS (see the *Messenger* No. 33 for a description of the prototype) has been used at the Cassegrain focus of the 3.6 m telescope. With this instrument,

the light of up to 54 objects in a field of 33' diameter is guided by fibers to the slit of a modified B&C spectrograph. A CCD is used as a detector. In the three test nights, the instrument operated smoothly on 8 fields and more than 300 objects were successfully observed.

OPTOPUS will be offered to the users as of October 1, 1985.



The giant and the midget: both attractive in their own way. In this picture, taken in the ESO Photolab, an OPTOPUS plate with holes to fit the optical fibers is shown close to a much smaller plate to be mounted on the EFOSC aperture wheel. Both combinations sample targets for multi-object spectroscopy at the Cassegrain focus of the 3.6 m telescope.

EFOSC, the ESO Faint Object Spectrograph and Camera, has also a multi-object spectroscopic mode (see the *Messenger* No. 38 for a description of the instrument).

A file containing the coordinates needed to punch an aperture plate can be created by identifying the targets on a CCD frame (5×3 arcminutes in size) obtained with the same instrument. Up to 11 plates can be mounted at one time on the EFOSC aperture wheel. In the March test, a plate with holes

corresponding to positions of peculiar H II regions in M 83 was prepared in the La Silla workshop and used successfully in the following night.

This observing mode will be offered to the users as of April 1, 1986.

A detailed description of the results of the tests and the operating manuals of OPTOPUS and EFOSC will be available by next fall. S. D'Odorico

Submillimetre Spectroscopy on La Silla

E. Krügel and A. Schulz, Max-Planck-Institut für Radioastronomie, Bonn

1. Of Pearls and Swine

Who would play a Stradivari violin at a country dance? Or who would mix very old Scotch with Coca-Cola? Not us. But we do things that look equally improper in the eyes of many astronomers. We employ fine optical telescopes to observe at submillimetre wavelengths, although for our purposes the surface accuracy of the mirror could be 1,000 times worse. One excuse which we (and the ESO Observing Programmes Committee) can offer is that at present there are no submillimetre telescopes that we could use instead of the optical ones. We believe that one can get information about star-forming regions through submillimetre observations that cannot be obtained by other means. This article is an attempt to convince you that this is the case.

2. The Value of Submillimetre Spectroscopy

There is a gap in observational astronomy between $20 \mu\text{m}$ and 1 mm that is only gradually beginning to be filled. This has two major causes. Firstly, the atmosphere is generally opaque because of water vapour and only in a few windows are observations possible from dry, high-altitude sites. La Silla is such a place. Secondly, up till a few years ago receiver technology at these wavelengths was not very advanced. However, all cold objects with temperatures below, say 50 K, emit predominantly at far infrared or submillimetre wavelengths. Molecular clouds are an example. H_2 , CO and more complicated species can form, if they are shielded by a few magnitudes of visual extinction from the energetic UV photons of the interstellar radiation field, which would otherwise dissociate the molecules. This shield is supplied by dust grains. Many of the astrophysically relevant atomic and molecular transitions lie in the submillimetre region. The whole problem of the early stages of star formation depends observationally on infrared and submillimetre astronomy, because protostellar clouds are completely opaque in the optical. While far infrared and submillimetre continuum measurements can determine the luminosity of a protostellar object, spectroscopic observations yield information on the kinematics of the gas, necessary to understand the collapse, and on the temperature and density structure as well.

CO is a key molecule in the study of the interstellar medium. It is abundant, easily excited and readily observed in its ground rotational transitions. They are labelled by their quantum number J of the upper and lower level. The lowest transition $J = 1-0$ occurs at 2.6 mm wavelength. It is always optically thick in the line centre. However, due to velocity shifts of the gas through turbulent and systematic motion one can also look into the cloud and detect the warmer and dense regions around embedded stars. The radiation of these young or even

pre-main-sequence stars is absorbed by the dust. The dust is at densities of more than 10^5 atoms per cm^3 thermally coupled to the gas and heats it. Such regions show an enhanced CO line temperature and are therefore called hot spots.

The J -th rotational level of CO lies $2.8 J(J+1)$ degrees Kelvin above the ground level. A comparable gas temperature is needed for its excitation. So in the CO ground transitions one mainly sees the cool gas away from the heating sources. For the study of star formation one wishes to penetrate as closely as possible to the protostar. The $J = 4-3$ line at 0.65 mm wavelength already needs an excitation of 55 K. Gas at such a temperature is found only in the vicinity of an embedded star. It is part of the protostellar cloud and its dynamics is dominated by the gravitational pull of the central object. The kinematics strongly influence the shape of the lines. Systematic motions which encompass the whole protostellar cloud, such as accretion, rotation or outflow, may be present together with chaotic or turbulent motions. Other effects, which are also

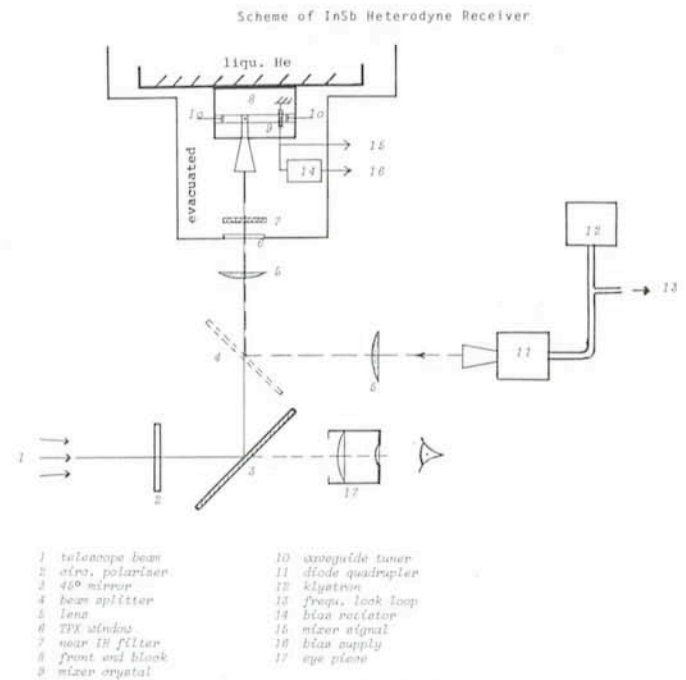


Fig. 1: Schematic drawing of the Indium Antimonide heterodyne mixer receiver (0.65 mm wavelength). The crystal sits within a front-end block with a horn antenna and a tunable waveguide circuit; its dimensions are $0.04 \times 0.04 \times 0.2$ mm. The local oscillator is a microwave klystron plus a Schottky diode quadrupler. Matching of the telescope beam to the beam shape of the horn antenna is done with lenses. The 45° mirror can be quickly exchanged by an eyepiece for optical pointing.

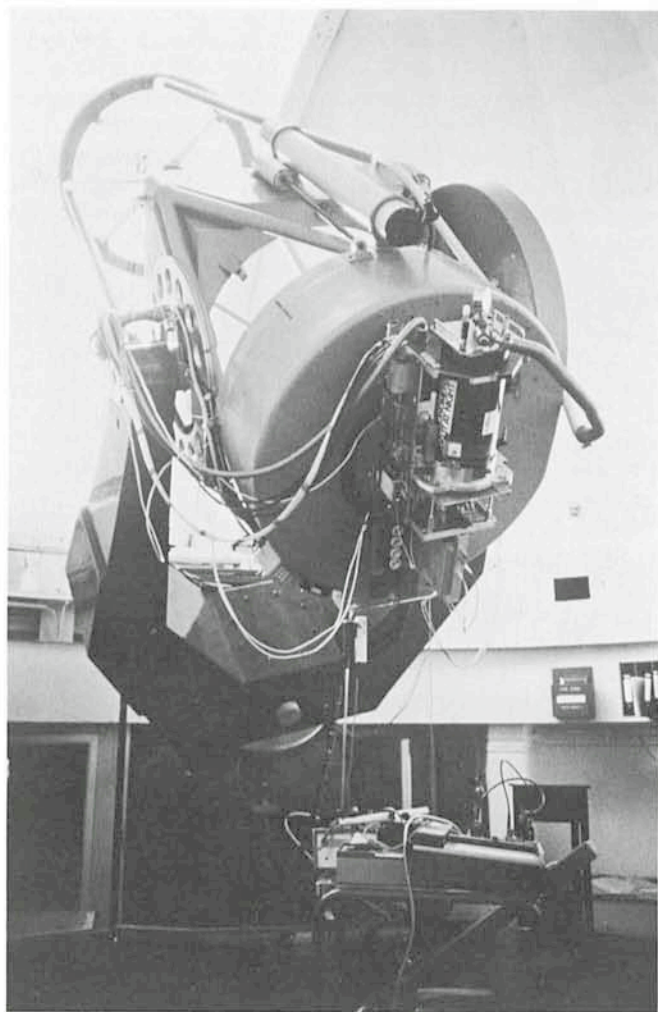


Fig. 2: Our Indium-Antimonide submillimetre receiver mounted on the ESO 1 m telescope. The tiny receiver crystal is mounted within the black Helium dewar (cooled to 2 K). The feed optics underneath the dewar cannot be seen, left of the dewar is the local oscillator plate; pipes are for pumping on the Helium.

important for the line shape, depend on the details of radiative transfer. For the submillimetre CO lines there is always the possibility of self-absorption in the line by cooler foreground material.

For a meaningful analysis of the CO cloud one has to combine the data of all lines available, including the optically thinner isotopic species. The most widely observed is $^{13}\text{C}^{16}\text{O}$, which is about 80 times less abundant than ordinary $^{12}\text{C}^{16}\text{O}$. Therefore optical depth effects do not play such an important role. This greatly simplifies the interpretation of the isotope lines. Unfortunately, the ^{13}CO $J = 4-3$ line cannot be observed from the ground. Although only 5 per cent shifted in frequency relative to ^{12}CO , it does not fall into an atmospheric window.

3. The Receiver

Our system is an indium-antimonide (InSb) receiver. At its heart is a semiconducting InSb crystal cooled by liquid helium to 2 K. At that temperature the electrons are only weakly coupled to the crystal lattice. When they absorb submillimetre photons, they increase their mobility and thus the conductivity of the crystal. The radiation of the astronomical object is mixed with that of the local oscillator (LO). The system has the inherent disadvantage that the resulting intermediate frequency (IF) has a bandwidth of only 1.5 MHz. For spectroscopy

the LO therefore has to be scanned through a certain frequency range. We use a klystron as LO and multiply its frequency with a diode quadrupler. On the telescope we work at 460 GHz or 0.65 mm wavelength. Frequency drive telescope control, data storing and processing are done with our own Hewlett-Packard 1000 computer. Fig. 1 displays the receiver schematically. We typically observe at 70 frequency points spaced at 1.5 MHz and thus have a velocity resolution of 1 km/s. The frequency range is scanned through ten times for about 10 s each, before the telescope is switched between ON and OFF position. We do not employ a chopping mirror.

The receiver has a system temperature of 800 K. It is small and light and technically simple, when compared to the future generation of diode mixers. Very important for a new spectral range, the receiver has also been well tested on the telescope under astronomically realistic conditions. Submillimetre nights are rare, everywhere. According to the very incomplete weather statistics, at best 20 per cent of the time can be used. When the sky is good for submillimetre astronomy, the observer is naturally tempted not to "waste" time on testing the system, but to do proper astronomy. However, spectroscopy is treacherous. We found that out once, while our system had not been fully tested: Looking at the well-known infrared and outflow source IRC 10216, we believed to have detected a line. Strength, width and shape looked reasonable. However, as we learned later, it was not a line, but just an artifact caused probably by reflections in the dome. In the meantime we have debugged and improved the system so that we feel safe to trust the data now.

4. Happy Faces

In July 1983 we had been granted seven nights both on the 1 m and on the 3.6 m telescopes. Such generosity is necessary for submillimetre observations considering the weather risk and the effort that goes into the mission: Three astronomers, the authors and A. Gillespie, an indispensable technician, F. Lauter, plus 700 kg of equipment had to be flown to Chile. Gillespie is the man who deserves the credit for starting the project at our Max-Planck Institute in Bonn five

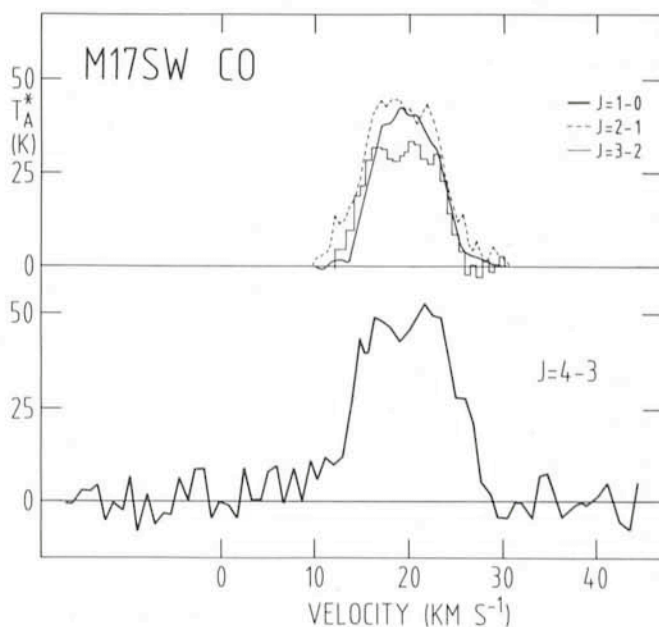


Fig. 3: Our spectrum (bottom) of the CO $J = 4-3$ line in IRC 1 located in the molecular cloud M17 SW. The top shows for comparison lower transitions observed with comparable resolution. References to them are given in Schulz et al. (1985, *Astron. Astrophys.*, in press).

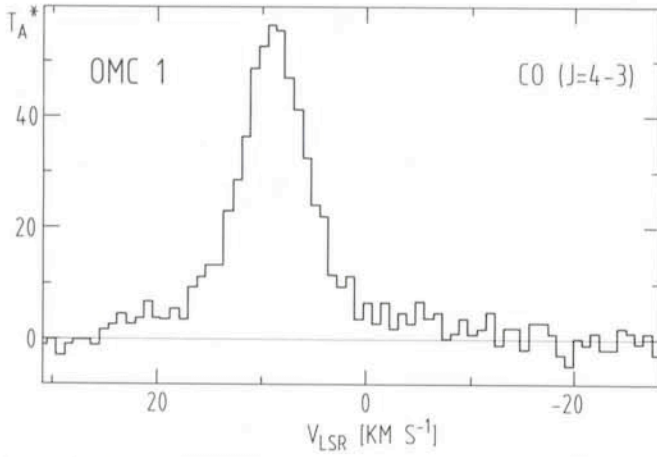


Fig. 4: The $J = 4-3$ transition of CO in the Orion nebula (OMC 1). Two distinct components of the line can be seen emitted by two different parts of the cloud: a narrow and bright spike and—due to a large velocity dispersion—a very broad pedestal (the line wings).

years ago. Meanwhile British industry has lured him away from astronomy.

The time on the 1 m was spent on testing the instrument (Fig. 2). On the 3.6 m we got two submillimetre nights; interestingly, they were not photometric. Only the extremely low humidity of 5% indicated a very low water absorption column. Up till then only Orion had been seen in the CO $J = 4-3$ transition. Of course, there must be other such sources in the sky, but we were not sure that we could detect them. Orion is exceptional in a number of ways. As hot spots, the regions emitting the CO $J = 4-3$ line might have a small angular diameter and pass undetected because of beam dilution. Orion was for us a morning object, so we started with the infrared source IRc 1 in the molecular cloud called M 17 SW. It lies south-west of the giant young H II region M 17. The lower

CO rotational transitions have their highest intensity towards IRc 1. We took our chance and were lucky. The detection was a gratifying experience; it was the first outside Orion. Now we know that this line is not uncommon and can be detected even with smaller telescopes at the price of lower spatial resolution. The spectrum of M 17 is shown in Fig. 3. Back in Bonn we constructed radiative transfer models for the propagations of the photons in the lines until our spectrum and those of the lower and isotopic ($^{13}\text{CO } J = 1-0$) transitions could be matched. The result was that the gas is not heated by the infrared object, which is probably a B0 star immersed in the molecular cloud, but by the O stars which excite the H II region. We concluded this because our models did not allow a temperature gradient in the cloud, as would be expected in the case of an internal heat source. We also found from the model that the gas does not have a systematic velocity, such as infall or outflow, but that it is highly turbulent and that the turbulence and the gas density peak towards IRc 1.

5. Outlook

CO submillimetre line observations have become possible only of late. One can expect them to give us clues about the environment of protostars. The $J = 4-3$ line is of particular interest. It comes from gas with temperatures which probably prevail in protostellar clouds. It also lies in an atmospheric window much less demanding than that of the next higher transitions ($J = 6-5, 7-6$), which are only observable from the ground under exceptional weather conditions. CO $J = 4-3$ spectroscopy will be a major activity with future submillimetre telescopes. Meanwhile we have to content ourselves with optical instruments.

To finally illustrate that one is already able to produce high quality measurements we present in Fig. 4 our spectrum of OMC 1: the plateau (broad wings) can clearly be seen. We hope that with such data we will be given another chance on La Silla.

Spectroscopy of Horizontal Branch Stars in NGC 6752

V. Caloi, Istituto di Astrofisica Spaziale, Frascati, Italy

1. Why a Globular Cluster

Globular clusters sit in the galactic halo as the most noticeable relics of the early epochs of galaxy formation. Being the oldest objects known and the only structured survivors of the complex initial galactic phases, they are the natural place where to look for information on the chemical composition of the matter emergent from the big bang (at least in first approximation).

One finds immediately that the heavy element (that is, elements heavier than helium) content is much in excess of what can be expected from a standard big bang nucleosynthesis. In fact, one observes in globular clusters a fraction by mass of elements from carbon on of at least $1.E-4$, against a predicted abundance of about $1.E-12$. Perhaps the easiest way to explain this pollution is in terms of globular cluster formation out of material enriched by the very first, metal-free stellar generations (Ref. 1).

At variance with what is believed for the heavy elements, the helium content in globular clusters is thought to be very close to the amount produced in the first three minutes of universal

expansion. This belief rests on the difficulty of making (or destroying) large amounts of helium in "normal" stars (Ref. 2). So globular cluster members are the natural targets for an investigation on primordial helium. The best candidates are, in principle, the unevolved main sequence stars, but, unfortunately, no helium line is observable in these cool objects. The low surface temperature prevents observation also in red giants, so that only hot horizontal branch (HB) stars (that is, on the left side of the RR Lyrae gap) give the opportunity for helium detection.

However, the situation is not straightforward even for these objects. First of all, they are faint or very faint: $V \geq 13.5$, so that only modern technology allows to reach them; secondly, it is necessary to know the effective temperature with good accuracy to obtain reliable abundances. This is a practically impossible task on the basis of observations in the U, B and V domains only; in fact, we are dealing with stars with effective temperatures of $15,000^\circ\text{K}$ or more, for which the peak of emission falls below 2000 \AA .

2. Why NGC 6752

This cluster is especially interesting. It exhibits the most developed blue “horizontal” (actually vertical) branch known at present (Fig. 1), with no RR Lyrae variables. It is therefore a good example of the so-called “second parameter” problem, which consists in a violation of the general rule for HB morphology: “the lower the heavy element abundance, the bluer”. On the contrary, NGC 6752 has more heavy elements than clusters such as M15 or M92, which have much shorter HBs with a not negligible population of RR Lyrae variables. (See Refs. 3 and 4 for reviews on globular clusters.)

Since so much of our knowledge on the early phases of the universe rests on an understanding of globular cluster evolutionary status, an exhaustive investigation of this peculiar cluster, with special reference to the HB problem, was started by a group of astronomers from several European institutions. The cluster is being studied from many points of view: (i) a statistically significant C-M diagram (Ref. 5); (ii) spectra in the optical range for HB stars obtained from ESO and AAT telescopes, analysed through synthetic spectra procedures (Refs. 6 and 7); and (iii) spectra in the far UV by means of the IUE satellite to finally overcome the difficulty in temperature determination for hot HB stars (Refs. 6 and 7).

Until now, almost 20 HB star spectra in the optical range and with intermediate dispersion have been obtained (mostly at the ESO 3.6 m telescope); 8 of these stars have been observed with IUE, mostly in the SW range (1200 Å–2000 Å). Incidentally, the SWP spectrum for the faintest object – $V = 17.76$ – ever observed with IUE was probably obtained in the course of this programme.

Fig. 2 exemplifies the procedure to achieve a reliable evaluation of effective temperatures for stars with an IUE spectrum.

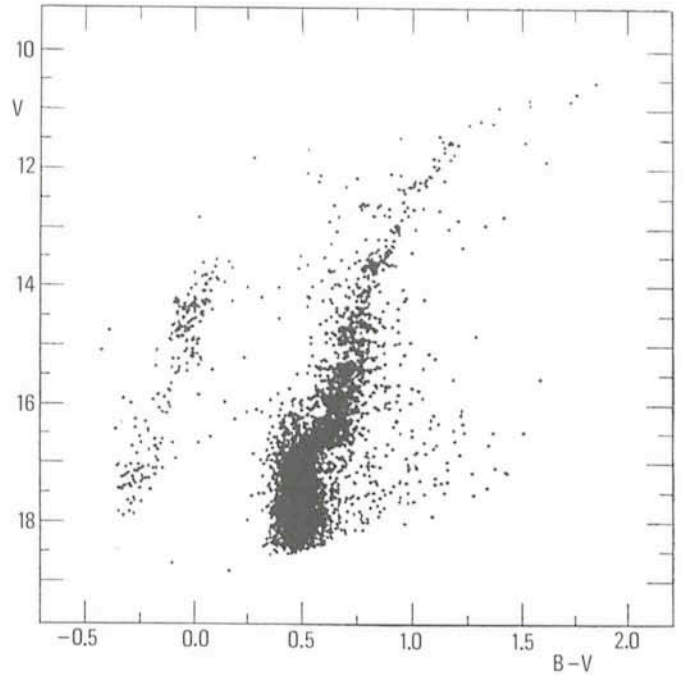


Fig. 1: The C-M diagram for NGC 6752 recently obtained by Buonanno et al. (Ref. 5). Note the exceptionally developed “horizontal” branch that stretches below the turn-off magnitude: a unique case up to now.

When the absolutely calibrated SWP spectrum is fitted to the V magnitude and is compared to theoretical predictions from stellar model atmospheres (Ref. 8), the effective temperature

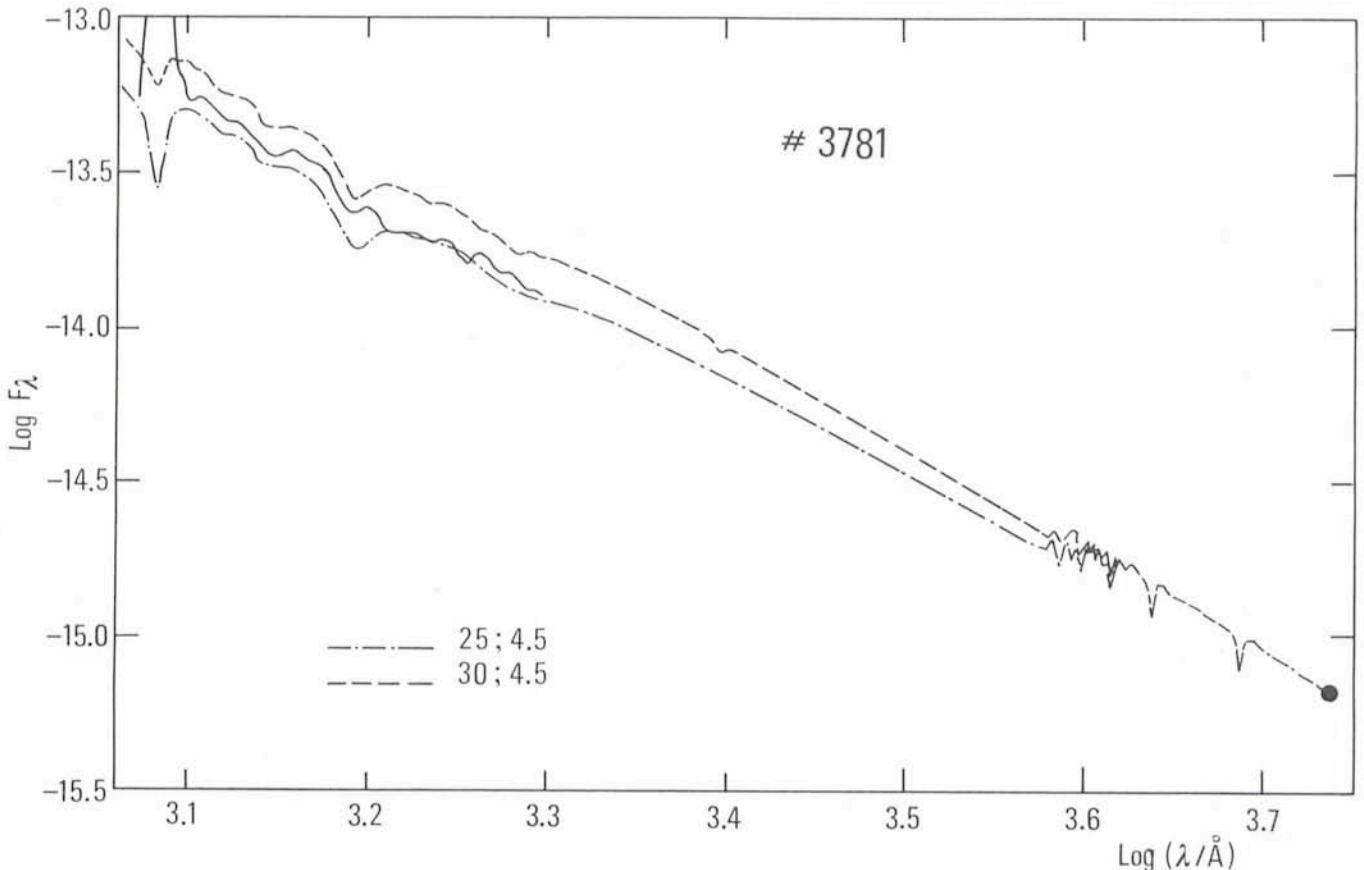


Fig. 2: By fitting IUE spectra to the observed V magnitude, reliable evaluations of effective temperatures are obtained. The dot indicates the flux corresponding to the visual magnitude; the IUE SWP spectrum (after rebinning in bands of 40 Å) is also shown (continuous line). The two comparison spectra are taken from Kurucz model atmospheres at the indicated temperatures (in units of 1000°K) and gravities (logarithm of).

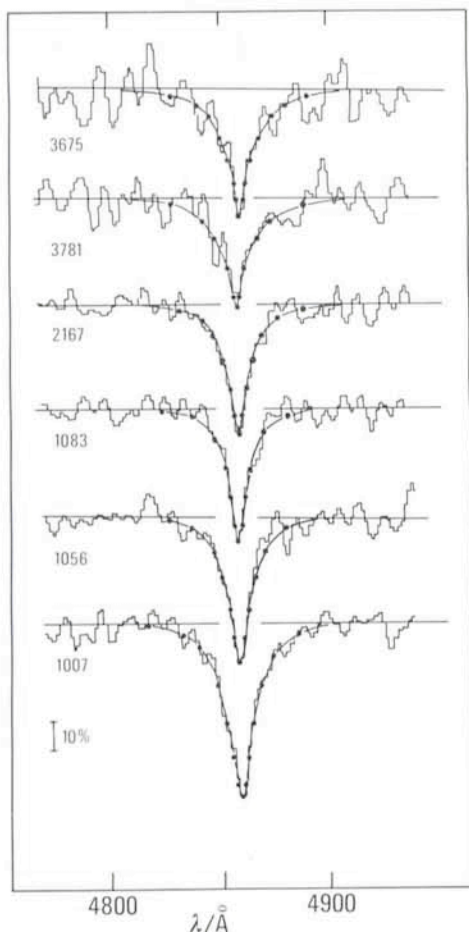


Fig. 3: Theoretical line profiles fitted to the observed Balmer lines in hot HB members of NGC 6752. Once the effective temperature is known from IUE observations, gravity is determined through the detailed fits of $H\beta$ (in the figure), $H\gamma$ and $H\delta$.

(T_e) can be determined to within 1,500°K or less. It is a very satisfactory accuracy for these objects, especially those with $V > 16$, which up to now were collectively classified as having T_e about 25,000°K.

The knowledge of T_e allows now a meaningful fitting of synthetic spectra to the observed hydrogen and helium lines. This work has been done by Uli Heber and R. P. Kudritzki (Ref. 7); Figs. 3 and 4 show some of the results, which have been quite remarkable. For the first time, helium has been observed directly in Population II stars and, besides, there is convincing evidence that helium is depleted in the atmospheres of these objects. In fact, the helium abundances, Y , in the Table show a one-to-one relation with the value of surface gravity, as expected under the gravitational sedimentation hypothesis.

Star:	3-118	V:	17.76	Log G:	5.40	Y:	≤ 0.01
	3781		16.96		5.14		= 0.02
	2167		15.76		4.27		= 0.11
	1083		15.33		4.16		= 0.14

From these observations the lower limit for helium in Population II turns out to be Y (mass fraction) = 0.14. Current estimates give a higher value for primeval helium, but we have to remember that it is likely that sedimentation is already acting in the hot ($T_e = 16,000^\circ\text{K}$) and condensed star # 1083.

So once again globular clusters confirm their importance as an "observational laboratory" where to check theories – and where to get new ideas – on stellar structure and evolution.

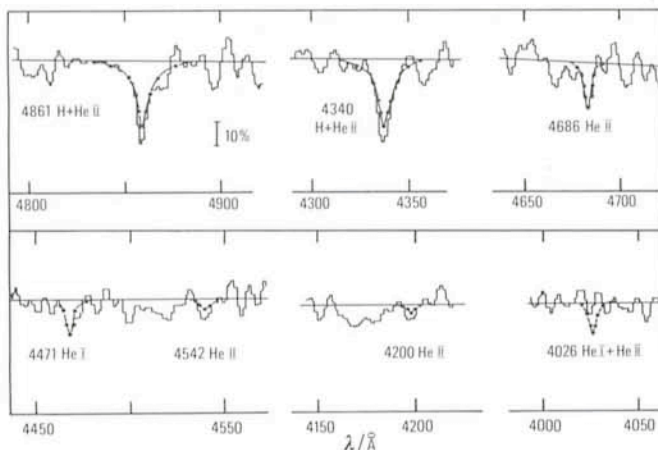


Fig. 4: Once effective temperature and gravity are known, helium abundance is obtained from the equivalent widths of selected helium lines.

Already observations with the instruments at our disposal, both ground and space based, are carrying us close to the heart of fundamental problems in stellar evolution; we are confident that the new technology telescopes and the Space Telescope will allow a qualitative, final jump.

References

1. Caloi, V. and Castellani, V. 1984, in *Frontiers of Astrophysics*, Ed. R. Pallavicini (Firenze), p. 97.
2. Arnett, W. D. 1978, *Astroph. J.* **219**, 1008.
3. Caloi, V. 1983, *Fund. Cosmic Physics*, **8**, 343.
4. Caputo, F. 1985, *Reports on Progress in Physics*, in press.
5. Buonanno, R., Caloi, V., Castellani, V., Corsi, C. E., Fusi Pecci, F. and Gratton, R. 1985, in preparation.
6. Caloi, V., Castellani, V., Danziger, J., Gilmozzi, R., Cannon, R. D., Hill, P. W. and Boksenberg, A. 1985, preprint.
7. Heber, U., Kudritzki, R. P., Caloi, V., Castellani, V., Danziger, J., Gilmozzi, R. and Cannon, R. D. 1985, in preparation.
8. Kurucz, R. C. 1979, *Astroph. J. Suppl.* **40**, 1.

List of ESO Preprints (March – May 1985)

364. I.S. Glass and A.F.M. Moorwood: JHKL Properties of Emission-Line Galaxies. *Monthly Notices of the Royal Astronomical Society*. March 1985.
365. A.A. Chalabaev and J.P. Maillard: Near Infrared Spectroscopy of γ Cas: Constraints on the Velocity Field in the Envelope. *Astrophysical Journal*. March 1985.
366. M. Azzopardi and J. Breysacher: On the Number of W-R Stars in the Large Magellanic Cloud. *Astronomy and Astrophysics*. March 1985.
367. I.J. Danziger and E.M. Leibowitz: Optical Spectrophotometric Study of SNRs in the LMC. *Monthly Notices of the Royal Astronomical Society*. March 1985.
368. D. Gillet, R. Ferlet, E. Maurice and P. Bouchet: The Shock-Induced Variability of the $H\alpha$ Emission Profile in Mira. II. *Astronomy and Astrophysics*. April 1985.
369. A. Pospieszalska-Surdej and J. Surdej: Determination of the Pole Orientation of an Asteroid: The Amplitude-Aspect Relation Revisited. *Astronomy and Astrophysics*. April 1985.
370. A.C. Danks and D.L. Lambert: The Chromospheric He I D_3 Line in Main-Sequence Stars. *Astronomy and Astrophysics*. April 1985.
371. E.J. Zuiderwijk: The Gravitational Lens Effect and the Surface Density of Quasars Near Foreground Galaxies. *Monthly Notices of the Royal Astronomical Society*. April 1985.
372. F. Matteucci and M. Tosi: Nitrogen and Oxygen Evolution in Dwarf Irregular Galaxies. *Monthly Notices of the Royal Astronomical Society*. April 1985.
373. B. Barbanis: Evolution of Families of Double- and Triple-Periodic Orbits. *Celestial Mechanics*. May 1985.

Visible and Infrared Study of L.P.V. with the 1 m Telescope

P. Bouchet and Th. Le Bertre, ESO, La Silla

Introduction

Long-period variables (L.P.V.) are evolved stellar objects whose luminosity varies with period ranging from ~ 100 to

$\sim 2,000$ days. The central stars are giants or supergiants with relatively low effective temperature (from 1,500 to 4,000°K). Depending on the abundance ratio (C/O), they are classified as carbon-rich (C/O >1) or oxygen-rich (C/O <1). Most of them

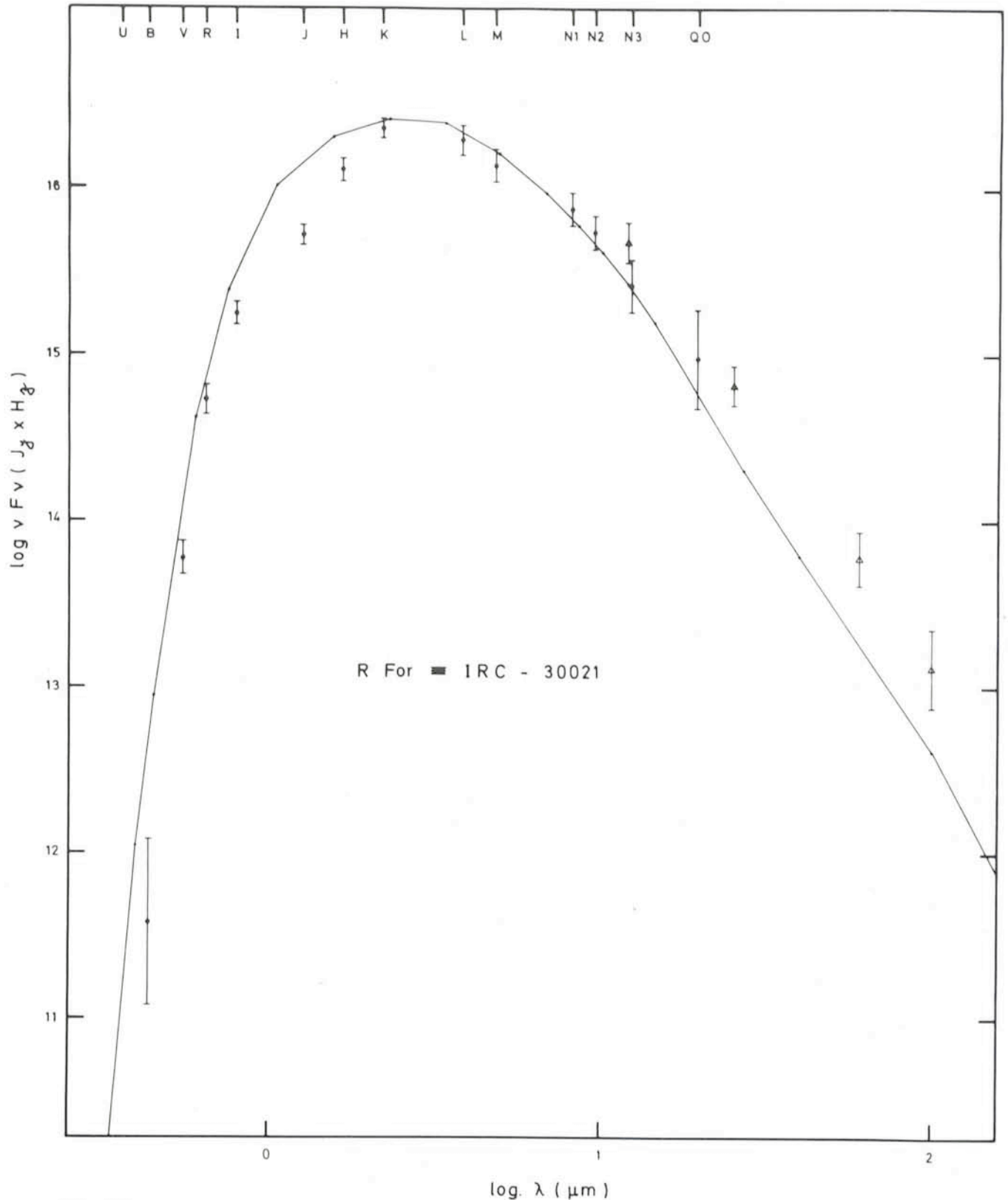


Fig. 1: Energy distribution of IRC-30021 between .4 and 1 μm . The dots correspond to photometric data obtained with the 1 m telescope and the triangles to IRAS data. The solid curve represents a numerical adjustment using a model described in the text.

are surrounded by a shell of gas and dust. When in the stellar atmosphere, carbon is more abundant than oxygen, all the oxygen is locked into carbon monoxide (CO), and the most probable species to condense out of the gas are made of carbon; consequently, the dust in the circumstellar shell will be mainly silicon carbide and graphite (or amorphous carbon). But if the star is oxygen-rich, all the carbon will be bound into CO, and the dust in the shell will be made of silicate (Salpeter, 1974). This circumstellar dust absorbs the stellar flux, and re-emits it at longer wavelengths. The optical thickness of the shell may be very great, to the point that, in some cases, the star is completely hidden inside its envelope.

High spectral resolution in the visible has revealed that these shells are expanding (Deutsch, 1956). Part of this expansion may be due to radiation pressure on the grains: grains are expelled by the absorption of stellar light and drag with them the circumstellar gas. This shell expansion is the manifestation of a mass-loss phenomenon. The study of this phenomenon is of importance as it affects the evolution of the central star; also, through it, these objects may be a major

source of matter for the interstellar medium. To tackle these questions and to get quantitative information, we have undertaken a photometric study of some L.P.V. We will illustrate this study with two objects that we are observing since October 1982, at La Silla, with the 1 m telescope.

R For:

This carbon star is a Mira of period ~ 400 days. When observed at the eyepiece, it presents a marvellous garnet colour due to the shape of its spectrum in the optical range (Fig. 1); the steepness in the blue is mainly due to absorption bands of C_2 and CN. Its infrared counterpart is a bright source discovered by Neugebauer and Leighton (1969) in their Two Micron Sky Survey (T.M.S.S.), where it is referred to as IRC -30021. Nevertheless, it has been little studied since that time.

We are obtaining (U,B,V,R,I) data using the 1 m ESO photometer equipped with the Quantacon, (J,H,K,L,M) data with the conventional 1 m infrared photometer and an InSb detector, and (M1, M2, M3 Q0) data with the same infrared photometer, but with a Ge-Ga bolometer. All our data presented in Fig. 1

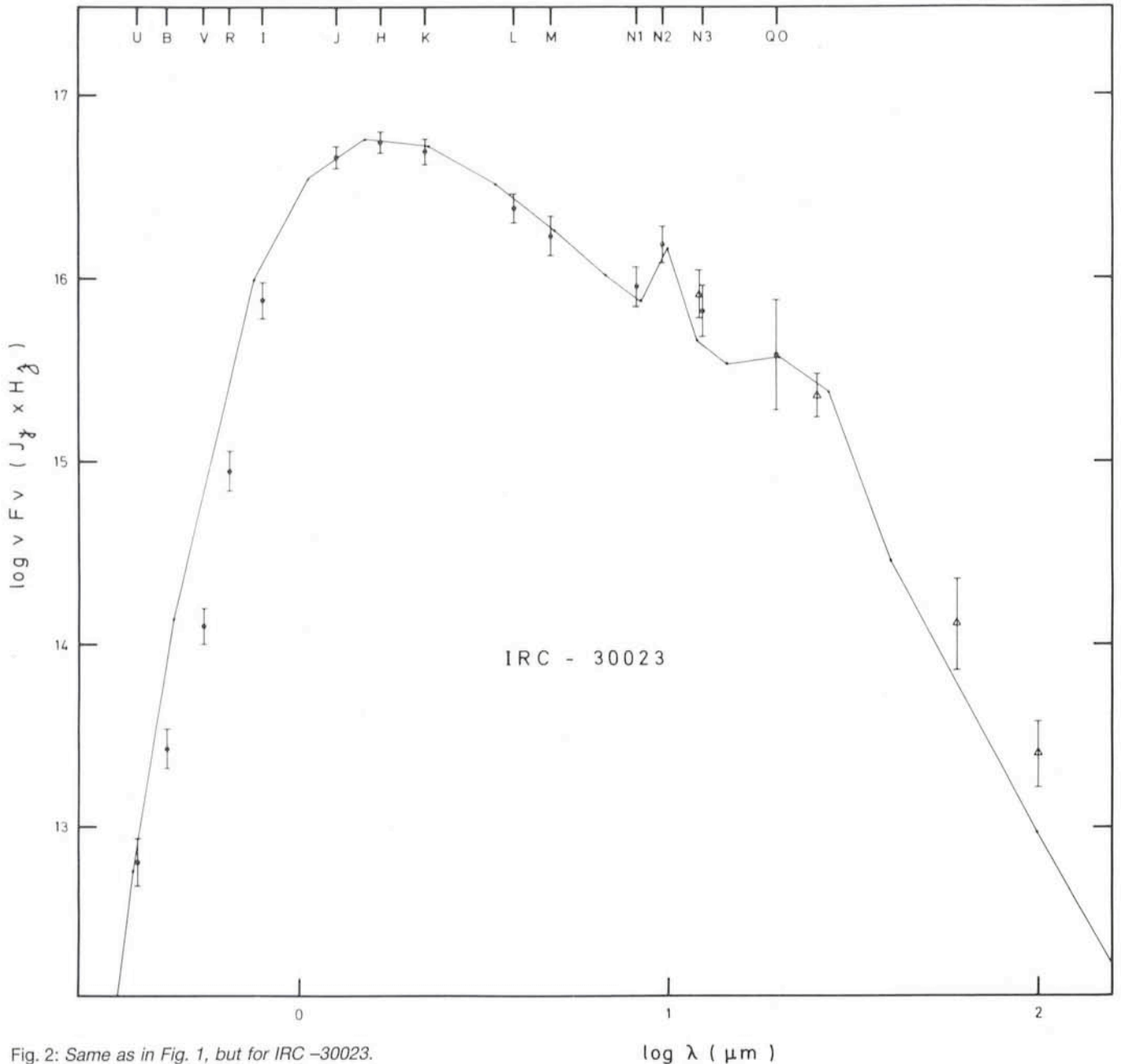


Fig. 2: Same as in Fig. 1, but for IRC -30023.

TABLE 1

Parameter	C / O > 1		C / O < 1	
	IRC -30021	GL 3068	IRC -30023	OH 353.60-0.23
d (kpc)	0.5	1.2	0.5	9.9
V_e (km s ⁻¹)	10	15	10	18
T_* (K)	2900	2000-3000	2200	2000-3000
$\tau_{10 \mu\text{m}}$	0.02	3.2	0.1	6.0
T_c (K)	1100	1600	750	900
\dot{M} ($M_\odot \cdot \text{yr}^{-1}$)	1.4×10^{-7}	3×10^{-5}	1.7×10^{-7}	6×10^{-5}
L_* (L_\odot)	3.6×10^3	17×10^3	7.3×10^3	80×10^3

Star and shell parameters deduced from adjustments of broad-band photometric data.

"d" is the object distance; " V_e ", the shell expansion velocity, " T_* ", the central star effective temperature; " $\tau_{10\mu\text{m}}$ ", the optical depth of the dust shell at 10 μm ; " T_c ", the condensation temperature of the dust; " \dot{M} ", the mass loss rate and " L_* ", the total luminosity.

are obtained at about the same phase, around December 20, 1984. We have plotted also, for comparison, at 12 and 25 μm , and for complementarity, at 60 and 100 μm , the data obtained by the IRAS satellite through 1983. As these data are not obtained at the same phase, there is a possible slight shift between them and ours.

The broad-band spectrum of IRC -30021 is featureless and looks like the one of a blackbody of temperature $\sim 1,200^\circ\text{K}$. Nevertheless, from its spectral type, the star effective temperature should be greater than 2,400 K. All this indicates the presence of carbon grains around R For; except for a resonance band around 11.5 μm which could be due to silicon carbide (SiC) these grains have optical characteristics which present no distinctive feature at $\lambda > .4 \mu\text{m}$.

We have developed a model of circumstellar dust shell based on the Leung (1975) radiative transfer method. Using the opacities derived by Jones and Merrill (1976) for graphite grains of radius $\sim 0.05 \mu\text{m}$, supposing that the central star radiates like a blackbody and assuming spherical symmetry and uniform expansion for the dust shell, we are able to adjust the observed data between .4 and 100 μm (solid line on Fig. 1). In this simplified model, we do not take into account photospheric bands due to CH, C₂, CN, CO, etc. and circumstellar bands mainly due to CO, in such a way that, in the observations, there is a strong deficit in B (CN and C₂), and also in J and H (CO, ...), with respect to the simulation. From this adjustment, we derive for R For, at .5 kpc, a stellar luminosity of $3 \times 10^3 L_\odot$ and a dust mass loss rate of $\sim 1.4 \times 10^{-9} M_\odot/\text{year}$ (or, adopting a gas-to-dust mass ratio of 100, a total mass loss rate of $\sim 1.4 \cdot 10^{-7} M_\odot/\text{year}$).

IRC -30023:

Very near IRC -30021, there is another bright infrared source discovered during the T.M.S.S.: IRC -30023. Our photometric data show it to be variable with a period of ~ 500 days. Although it has an optical counterpart which may be quite bright ($V \sim 10$ near maximum), till now, it has not been catalogued as a variable star. Fig. 2 presents its broad band spectrum between .4 and 100 μm . A strong emission feature, visible at 10 μm , indicates the presence of silicate dust in a circumstellar shell. We infer from it that the central star is oxygen-rich.

As for IRC -30021, we performed the modeling of this dust shell, using now opacities of silicate grains of radius $\sim .1 \mu\text{m}$. The solid line in Fig. 2 presents our adjustment. Photospheric absorption bands (mainly due to TiO) are not taken into account in our model and their effects can be seen on the B, V, R fluxes. Our fit implies a total luminosity of $\sim 7 \times 10^3 L_\odot$ and a total mass loss rate of $\sim 1.7 \times 10^{-7} M_\odot/\text{year}$.

Conclusion

We are studying at the 1 m telescope a whole sample of evolved stars with luminosities ranging from $\sim 10^3$ to $\sim 10^5 L_\odot$ and mass loss rate from 0 to $10^{-4} M_\odot/\text{year}$; a few results are given in Table 1. As these objects are variable, it is very important to monitor them for investigating their evolution, and for evaluating their importance in the replenishment of the interstellar medium.

As it is equipped with visible and infrared photometers, the 1 m telescope is very adequate for this kind of study. Its excellent pointing and tracking accuracy makes it particularly valuable for photometry, to the point that, as long as there is not too much turbulence, infrared observations can be performed even during the day. This quality is especially useful for monitoring variable objects of period \sim one year or more.

References

- Deutsch, A. J.: 1956, *Astrophys. J.* **123**, 210.
 Jones, T. W. and Merrill, K. M.: 1976, *Astrophys. J.* **209**, 509.
 Leung, C. M.: 1975, *Astrophys. J.* **199**, 340.
 Neugebauer, G. and Leighton, R. B.: 1969, NASA SP-3047.
 Salpeter, E. E.: 1974, *Astrophys. J.* **193**, 579.

STAFF MOVEMENTS

Arrivals

Europe

- AURIERE, Michel (F), Fellow
 GILLI, Bruno (F), Programmer
 SCHARRER, Rebekka (D), Laboratory Technician (Photography)
 STAHL, Otmar (D), Fellow
 WAMPLER, Joseph (USA), Scientist

Chile

- MULLER, Guido (CH), Electro-mechanical Engineer
 VAN DEN BRENK, John (Australia), Detector Engineer

Departures

Europe

- LECLERCQZ, Jean (B), Draughtsman (Graphics)
 PAUREAU, Jean (F), Mechanical/Cryogenics Engineer

Chile

- DANKS, Anthony (GB), Astronomer

ESO, the European Southern Observatory, was created in 1962 to... establish and operate an astronomical observatory in the southern hemisphere, equipped with powerful instruments, with the aim of furthering and organizing collaboration in astronomy... It is supported by eight countries: Belgium, Denmark, France, the Federal Republic of Germany, Italy, the Netherlands, Sweden and Switzerland. It operates the La Silla observatory in the Atacama desert, 600 km north of Santiago de Chile, at 2,400 m altitude, where thirteen telescopes with apertures up to 3.6 m are presently in operation. The astronomical observations on La Silla are carried out by visiting astronomers – mainly from the member countries – and, to some extent, by ESO staff astronomers, often in collaboration with the former. The ESO Headquarters in Europe are located in Garching, near Munich. ESO has about 135 international staff members in Europe and Chile and about 120 local staff members in Santiago and on La Silla. In addition, there are a number of fellows and scientific associates.

The ESO MESSENGER is published four times a year: in March, June, September and December. It is distributed free to ESO personnel and others interested in astronomy.

The text of any article may be reprinted if credit is given to ESO. Copies of most illustrations are available to editors without charge.

Technical editor: Kurt Kjær

EUROPEAN
SOUTHERN OBSERVATORY
Karl-Schwarzschild-Str. 2
D-8046 Garching b. München
Fed. Rep. of Germany
Tel. (089) 32006-0
Telex 5-28282-0 eo d
Telefax: (089) 3202362

Printed by Universitätsdruckerei
Dr. C. Wolf & Sohn
Heidemannstraße 166
8000 München 45
Fed. Rep. of Germany

ISSN 0722-6691

ESO Video Film Now Available

We are happy to announce that a 24-minute video film about ESO is now available. It was made by ESO staff in collaboration with a professional producer and shows scenes from La Silla and Garching. The structure of ESO is explained and the work, both astronomical and technical, is illustrated. Since this is the first film which has been specifically made to "present" ESO to the public in the member states and beyond, the level is such that no particular knowledge about astronomical science and technology is required by the audience. The film is therefore also suitable for schools, astronomical amateur clubs, planetaria, etc.

In order to facilitate the comprehension, the film is available in eight languages: Danish, Dutch, English, French, German, Italian, Spanish and Swedish. It can be obtained on VHS, V2000, Betamax and other common video systems.

The film can be obtained from: ESO Information Service, Karl-Schwarzschild-Straße 2, D-8046 Garching, Fed. Rep. of Germany.

The price is DM 70,-, including mailing costs.

ALGUNOS RESUMENES

Dos opciones para espectroscopia simultánea de varios objetos con el telescopio de 3,6 m

En marzo se probaron con éxito en La Silla dos instrumentos para obtener espectros de varios objetos en un campo con una sola exposición.

Se usó una versión mejorada del OPTOPUS en el foco Cassegrain del telescopio de 3,6 m. Con este instrumento, da luz de hasta 54 objetos, en un campo de 33' de diámetro, es guiada por fibras a la ranura de un espectrógrafo B&C modificado. Se usa un CCD como detector. Durante las tres noches de prueba el instrumento funcionó sin problemas en 8 campos y se observaron más de 300 objetos con éxito.

El OPTOPUS será ofrecido a los usuarios a partir del 1° de octubre de 1985.

EFOSC, espectrógrafo y cámara ESO para objetos débiles, se puede operar también en modo espectroscópico múltiple. Un archivo, que contiene las coordenadas necesarias para perforar una placa de apertura, puede ser creado por medio de la identificación de objetos en una imagen CCD (con una dimensión de 5 x 3 minutos de arco) obtenidos con el mismo instrumento. Se pueden montar hasta 11 placas a la vez en la rueda de apertura del

EFOSC. Para la prueba en marzo se preparó en el taller de La Silla una placa con perforaciones que corresponden a las posiciones de regiones peculiares HII en M83 y ésta fue usada con éxito la noche siguiente.

Este modo de observación será ofrecido a los usuarios a partir del 1° de abril de 1986.

R136a resuelto por interferometría «speckle» holográfica

R136 es el misterioso objeto central de la nebulosa 30 Doradus en la Gran Nube Magallánica. Este objeto tiene una componente brillante, R136a, y dos componentes más débiles, R136b y R136c. En el pasado existían principalmente dos opiniones sobre la naturaleza de R136a: o que fuera un objeto supermasivo con una masa de aprox. 1000 a 3000 masas solares o un cúmulo denso de estrellas O y WR.

Ahora los Sres. Weigelt, Baier y Ladebeck fueron capaces de resolver el objeto por medio de interferometría «speckle» holográfica. La figura 2 en página 5 muestra la primera imagen de R136a verdaderamente limitada por difracción. Esta imagen demuestra que R136a es un denso cúmulo que contiene por lo menos 8 estrellas. Los objetos dominantes en R136a son las tres estrellas brillantes R136 a1, a2 y a3 que tienen casi idénticas magnitudes. Las separaciones de a1-a2 y a1-a3 son de 0.10 y 0.48 segundos de arco, respectivamente.

Contents

M. Mayor and G. Meylan: Radial Velocities of Stars in Globular Clusters: a Look into ω Cen and 47 Tuc	1
Tentative Time-table of Council Sessions and Committee Meetings in 1985	3
G. Weigelt, G. Baier and R. Ladebeck: R136a and the Central Object in the Giant HII Region NGC 3603 Resolved by Holographic Speckle Interferometry	4
Access to IRAS Data in ESO Member Countries	6
W.F. Wargau: Nova-like Objects and Dwarf Novae During Outburst – A Comparative Study	7
S. D'Odorico: Two Multi-Object Spectroscopic Options at the ESO 3.6 m Telescope ..	11
E. Krügel and A. Schulz: Submillimetre Spectroscopy on La Silla	12
V. Caloi: Spectroscopy of Horizontal Branch Stars in NGC 6752	14
List of ESO Preprints (March – May 1985)	16
P. Bouchet and Th. Le Bertre: Visible and Infrared Study of L.P.V. with the 1 m Telescope	17
Staff Movements	19
ESO Video Film Now Available	20
Algunos Resúmenes	20